



Université
de Toulouse

THÈSE

En vue de l'obtention du
DOCTORAT DE L'UNIVERSITÉ DE TOULOUSE

Délivré par :

Institut National Polytechnique de Toulouse (INP Toulouse)

Discipline ou spécialité :

Dynamique des fluides

Présentée et soutenue par :

Kaushik Kumar NAGARAJAN

le : lundi 8 février 2010

Titre :

Analysis and control of self-sustained instabilities in a cavity
using reduced order modelling

Analyse et contrôle des instabilités dans une cavité
par modélisation d'ordre réduit

JURY

Jean-Pierre RAYMOND, Professeur, Université Paul Sabatier, IMT, Toulouse, Président

Christophe AIRIAU, Professeur, Université Paul Sabatier, Toulouse, Directeur

Laurent CORDIER, Chargé de recherche CNRS, LEA/CEAT, Poitiers, Examineur

Angelo IOLLO, Professeur, Université Bordeaux, IMB, Bordeaux, Rapporteur

Bernd. R NOACK, Directeur de Recherche CNRS, LEA/CEAT, Poitiers, Rapporteur

Ecole doctorale :

Mécanique, Énergétique, Génie civil et Procédés (MEGeP)

Unité de recherche :

Institut de Mécanique des Fluides de Toulouse (IMFT)

Directeur(s) de Thèse :

Christophe AIRIAU, Professeur, Université Paul Sabatier, Toulouse

Azeddine KOURTA, Professeur, Polytech Orléans, PRISME, Orléans

Rapporteurs :

Angelo IOLLO, Professeur, Université Bordeaux, IMB, Bordeaux

Bernd. R NOACK, Directeur de Recherche CNRS, LEA/CEAT, Poitiers

Acknowledgments

Thomas Alva Edison once said: "100% Success = 99% perspiration + 1% inspiration" ! for me, the ratio of perspiration to inspiration didn't trigger my thoughts as much as the truth that inspiration is more dense, deeper and carries equal weight! Without being 'calculative' in expressing myself, I would still have to admit my anxiety of making understatements:

I cannot thank enough my supervisors Christophe Airiau and Azeddine Kourta who have motivated me to stretch my forte and my competence beyond limits and thereby helped me discover my inner strength which I was not aware of. I owe the success of my efforts and the brightness of my future to them. Christophe brought to this work the insight and rigor in many parts especially concerning 'Control'. I am very indebted to him for having instilled in me a sense of rigor in my research, as well as in presenting this work. His concern to make his students learn the state-of-art was very well ref ected in the many workshops I attended during the three years.

Words fail to express my gratitude to Laurent Cordier from LEA Poitiers, who has for the most part of the work served as a virtual supervisor. His knowledge in POD based Reduced Order Modelling was indispensable. His rigor and never-say-die attitude has rubbed off on me for life. He has held the guiding light for me to tread this path and has encouraged me all-through. His guidance and constructive criticism have been like stepping stones in the process. Thanks for his great patience in talking to me practically everyday and advising me. Apart from this, I enjoyed the moments of long discussions I had with him on almost every topic.

I sincerely thank Bernd Noack and Angelo Iollo for accepting to be a part of the jury. Their deep knowledge of the state-of-art was ref ected in the many questions they posed and has encouraged me to pursue this f eld further in my career. I would also like to thank Jean-Pierre Raymond for agreeing to preside over the defence presentation. I would also like to remember him for the good lunches I had at his home, his lively spirit and love for Mathematics. I would also like to acknowledge Professor Pierre Comte of LEA Poitiers for providing me with a copy of his DNS code and his help during the initial days of the work.

Thanks for the support I received from the Service Informatiques during the last three years. Special thanks to Nicolas Renon of CICT for providing me various tips on large-scale computation. Thanks to Marie Christiani secretary of the group for coordinating the various activities of the project. Her enthusiasm to help foreign students in many day-to-day activities is noteworthy. I would also like to thank Véronique Cassin, the new secretary, for her help during the last days of the work.

Special thanks to the various partners of the AeroTraNet project who gave a new direction on solving a problem by combining the various aspects of work like numerical, experimental. The bi-annual meetings gave me an unique opportunity to network with various researchers working on different aspects of the same problem. I would also like to thank peers in the f eld whom I met during many conferences and workshops. Thanks to Clancy Rowley, Dietmar Rempfer, Ravindran for providing many exciting perspectives of thought. A special acknowledgment goes to John Burkardt from Florida State University for maintaining the best collection of libraries of various programs which have been used in this work. I have copied his style of programming!

Thanks to Laia and Sivam, mes amies in this long sejour of three years, who have stood by me and encouraged all along. Laia has been a great support till the last days of my thesis. Her

uncanny ability to organise things leaves me awe-struck. Sivam by sharing his treasure of Tamil songs made my days lively. Thanks to my other friends Karim, Anais, Houssam, Remi, Wafa, Marguerite, Thibaud, Benjamin, Romain, Xavier, Rudy, Mariyana, Bernard, Dirk, Yannick, Marie, Omar, Luigi, Sheetal and Aalap for their support and encouragement. I would like to acknowledge Yogesh for suggesting many improvements in the write-up. Thanks to David for giving me various tips for my final presentation.

I owe my heart filled thanks to my parents; especially my mother (Smt. Girija Nagarajan), brother and sister-in-law (Ishwar & Ramya), sisters - Rani, Preethi, Gowri (Chinni included) for their encouragements, forbearance, support and prayers and having stood by me during 'high and low tides', for the unfaltering faith they had in me, which was an essential base to the victorious atmosphere I'm breathing in, right now.

Thanks to my friends the Badri-boys (Dilip, Guru, JP, Kiran, Parag, Sriram, Sreenidhi, Vivek), Divya and Swathi for their constant encouragement and prayers for my betterment. I would like to thank Raghoothamachar for cultivating in me a sense of unbiasedness while pursuing knowledge. Thanks to Dr. Ramesh (NAL) for encouraging me in my pursuits. I would also like to thank Dr Kirti Malhotra and Dr N. Balasubramanya my undergraduate professors. Thanks to Professor A.S.Vasudevamurthy of TIFR for his words of motivation to come abroad for a PhD.

There is no greater blessing than to have the guidance of an enlightened personality. All our knowledge, inspiration and wisdom are dormant within us as seeds. The proper watering through spiritual guidance nurtures these seeds to grow into deep-rooted, majestic trees. That kind of initiation is what I have received from Shrila Prabhupada. This seed was further cultivated and enriched by Shri Bannanje Govindacharya by showing me a new light, leading to the path of Shri Madhwacharya, who is immanent in every soul, the preceptor of all the worlds and the embodiment of all virtues.

Last but not the least, all these thanks-giving would have no real meaning if I fail to recognise the Supreme Lord Shri Krishna, immanent in all of them. I humbly dedicate this work unto His lotus feet with heart-felt prayers. I would like to admit that I too am a mere instrument in this progression.

This thesis has been supported by a Marie Curie Early Stage Research Training Fellowship of the European Community's Sixth Framework Programme under contract number MEST CT 2005 020301.

Contents

General Introduction	1
1 Description and validation of the numerical tool	7
1.1 Introduction	10
1.2 Non-dimensionalisation parameters	10
1.3 Governing equations in cartesian coordinate system	11
1.4 Time advancement	12
1.5 Boundary conditions	13
1.5.1 Wall boundary condition	13
1.5.2 Non-reflective boundary conditions	13
1.5.3 Subsonic inflow boundary condition	15
1.5.4 Subsonic non-reflecting outflow boundary condition	16
1.6 Modelling cavity flows using NIGLO	17
1.7 Introduction of control	21
1.8 Conclusion	23
2 Basic tools from control theory	25
2.1 Introduction	28
2.2 Open loop control and constrained optimisation	29
2.2.1 Functional gradients through sensitivities	34
2.2.2 Functional gradients using adjoint equations	34
2.2.3 Differentiation then Discretisation	35
2.2.4 Discretisation-Differentiation	35
2.2.5 Differentiation-Discretisation	35
2.3 Feedback control	37
2.4 \mathcal{H}_2 control theory	38
2.4.1 Linear Quadratic Regulator LQR control	38
2.4.2 Lyapunov equation and minimum of the functional \mathcal{J}_{LQR}	39
2.4.3 Estimation and the Kalman-Bucy Filter (KBF)	40
2.4.4 Linear Quadratic Gaussian LQG control	43
2.5 \mathcal{H}_∞ control: robust control	44
2.6 Conclusions	46

3	Proper Orthogonal Decomposition (POD) based Reduced Order Modelling (ROM)	47
3.1	Introduction	53
3.2	Reduced order modelling an overview	53
3.2.1	Historical background of POD	54
3.2.2	Application of POD in control and turbulence	55
3.3	Proper Orthogonal Decomposition	55
3.4	Properties of POD	57
3.5	Finite dimensional case	60
3.6	Singular Value Decomposition (SVD)	62
3.6.1	Geometric interpretations of SVD	62
3.6.2	Connection between the SVD and eigenvalue problems	63
3.7	Direct and snapshot method	64
3.7.1	On the application of the classical eigenvalue problem:	64
3.7.2	Snapshot POD	65
3.8	Choice of inner product	66
3.8.1	L^2 inner product	67
3.8.2	H^1 inner product	67
3.8.3	Compressible inner product	67
3.9	ROM in literature	68
3.10	Galerkin projection, principles	69
3.11	Incompressible case	70
3.12	Compressible case	72
3.13	Extension to actuated case	73
3.13.1	Reduced order model for the actuated case	75
3.13.2	A polynomial notation for the reduced-order model	77
3.13.3	Extension to multiple modes	78
3.14	Application to cavity flows	80
3.15	Conclusion	82
4	Integration and calibration of ROM	89
4.1	Introduction	92
4.2	Definition of errors	93
4.2.1	State calibration method with nonlinear constraints	93
4.2.2	State calibration method	94
4.2.3	Flow calibration method	94
4.2.4	Affine function of error	95
4.3	Calibration method of Couplet	96
4.4	Application to cavity flow	97
4.4.1	Introduction	97
4.4.2	Minimisation of $\mathcal{J}_\alpha^{(2)}$ and $\mathcal{J}_\alpha^{(3)}$	98
4.5	Calibration by the method of Tikhonov regularization	101
4.5.1	Filter factors and Picard's criteria	101

4.5.2	Tikhonov regularization	102
4.5.3	A weighted approach to Tikhonov regularization	105
4.5.4	Comparison of different types of Tikhonov regularization	108
4.6	Comparison with other calibration methods	111
4.7	Long time time integration of the POD ROM	112
4.8	Conclusion	113
5	Feedback control of cavity f ows	115
5.1	Introduction	117
5.2	Tools used for the feedback design	117
5.2.1	<u>L</u> inear <u>S</u> tochastic <u>E</u> stimation (LSE)	118
5.2.2	Sensitivity analysis of the actuated terms	119
5.2.3	Linearisation of the plant	121
5.3	Feedback design.	124
5.3.1	Controller	124
5.3.2	Observer	125
5.3.3	Simulation of the full system	125
5.3.4	Application to cavity	126
5.4	Conclusion	130
	Conclusions and Perspectives	133
	Annexes	141
A	Controllability and observability of linear systems	141
B	Galerkin projections for the full NS equations	143
C	Specific volume formulations of ROM	145
D	Actuated POD by the method of stochastic estimation	147
E	Theorem concerning actuated mode	149
F	<u>G</u>eneralized <u>S</u>ingular <u>V</u>alue <u>D</u>ecomposition (GSVD)	153
G	Open loop control	155
G.1	Open loop control of cavity f ows	155
G.2	Resolving the optimal system	156
G.3	Open loop control of cavity	158
H	An open loop approach to handle the acoustic terms in ROM	161

General Introduction

Motivation

Les émissions acoustiques représentent un des problèmes majeures du transport aérien qui concernent l'environnement. Généralement on classe les bruits émis en fonction de leur origine mécanique, aérodynamique et ceux liés aux systèmes secondaires. On s'intéresse ici au bruit émis au voisinage des aéroports, et il provient pour l'essentiel (voir figures 1 et 2) de l'écoulement autour du train d'atterrissage, de celui des jets de réacteurs et de différentes cavités présentes sur l'avion. Nous allons dans la suite considérer uniquement la géométrie de la cavité dont l'écoulement est schématiquement donné sur la figure 3 et 4, en fonction du rapport d'aspect. Le travail présenté ici consiste à analyser la physique de l'écoulement et de la propagation du bruit et surtout à chercher à réduire les émissions acoustiques.

Différentes approches expérimentales par un contrôle passif ou actif de l'écoulement ont pu déjà être testées avec plus ou moins de succès, grâce en particulier aux avancées techniques dans les moyens de mesures et de contrôle, et dans le domaine des ressources informatiques. Actuellement, en utilisant les Simulations Numériques Directes (DNS) ou les Simulations à Grandes Echelles (LES) nous sommes en mesure de mieux comprendre la physique de cet écoulement. Par contre, compte tenu de l'énorme dimension du problème, les études numériques et théoriques du contrôle acoustique doivent nécessairement passer par la réduction de modèle (ROM, voir figure 5). Ici nous appliquerons la Décomposition en Valeurs Propres Orthogonales (POD), qui permettent finalement de réduire la complexité des équations de Navier-Stokes à la résolution et donc au contrôle, d'un système d'équations aux dérivées ordinaires (ODE, voir figure 6), plus simple à manipuler et résoudre. En se basant sur les travaux précédents de [Rowley et al. \(2003\)](#), [Gloerfelt \(2008\)](#), [Kasnakoğlu \(2007\)](#), [Samimy et al. \(2007\)](#) et de [Cordier et al. \(2009\)](#), nous allons proposer un contrôle du système réduit, une fois celui-ci calibré et l'appliquer ensuite sur le système complet issu des Simulations Numériques Directes.

Ce travail a été effectué dans le cadre d'un projet Marie-Curie appelé AeroTraNet, mené en collaboration avec 3 universités étrangères. Le LEA de Poitiers a largement contribué aux différentes parties: L. Cordier pour ce qui concerne la réduction de modèle, P. Comte pour les DNS.

Organisation du document

La chapitre 1 introduit l'outil de simulation numérique de base (DNS). Les éléments de la théorie du contrôle utilisés plus tard sont présentés dans le chapitre 2. Le chapitre suivant est consacré à la réduction de modèle et son application sur l'écoulement de cavité. Le système dynamique obtenu est fortement instable aussi le chapitre 5 est dédié à la calibration et la stabilisation du modèle réduit. De multiples approches sont abordées. Le contrôle du système dynamique forcé et son effet sur l'écoulement complet, sur la base de la théorie du contrôle linéaire quadratique gaussien sont finalement présentés dans le chapitre 5. Une conclusion suivi de quelques annexes achèvent le document.

Motivation

The recent rise in the air travel has given rise to a number of environmental concerns of which an important issue is the noise. Exposure to noise, particularly near the airports have been known to cause a number of health problems, like stress, hearing problems, hypertension, cardio-vascular problems, sleeping disorders. A constant exposure to noise levels beyond 65 – 70 dB is known to cause life term health effects.

Noise emitted from an aircraft can be broadly classified as mechanical noise, aerodynamic noise and aircraft system noise. Mechanical noise is usually caused due to propeller, jet engines. The main source of mechanical noise in an aircraft occurs during cruise conditions, due to the high velocity of jet from the engine. The aerodynamic noise arises due to the airflow around the different geometric configurations such as fuselages, high lift devices, landing gears, head and tail rotors of a helicopter etc. Aircraft system noise is mainly due to the cabin pressurisation as well as due to the auxiliary power units used to start the main engines, to provide power during ground conditions. Although during cruise conditions the mechanical noise dominates, the aerodynamic noise assumes an equal proportion during landing and takeoffs. Most of the aerodynamic noise during landing and take-offs can be associated to the landing gear, the geometry of which can be modelled as a cavity. Figure 1 shows the various components of noise sources during the landing or takeoff of aircrafts. Typical values of perceived noise, due to various components, during take off and landing is shown in figure 2.

A similar phenomenon can also be seen in other configurations such as weapon bays, joints between high speed train bogies, car body openings. This brings to interest the study of cavity flows, particularly when in search of quieter aircrafts as envisaged in the report European aeronautics: a vision for 2020 by [EC \(2001\)](#).

A typical cavity flow configuration is as shown in figure 3. The physics of the cavity can be explained by the formation of the shear layer at the upstream cavity edge. As the shear layer propagates it breaks down due to the Kelvin-Helmholtz mechanism resulting in a membrane like oscillation. The shear layer impinges the downstream edge of the cavity and splits, resulting in the formation of vortical structure close to the downstream edge, and is of the size of the depth of the cavity. This results in the formation of acoustic waves which propagates into the upstream, causing the far-field noise. The cavity can be classified based upon the flow mechanism it generates, as an open cavity or a closed

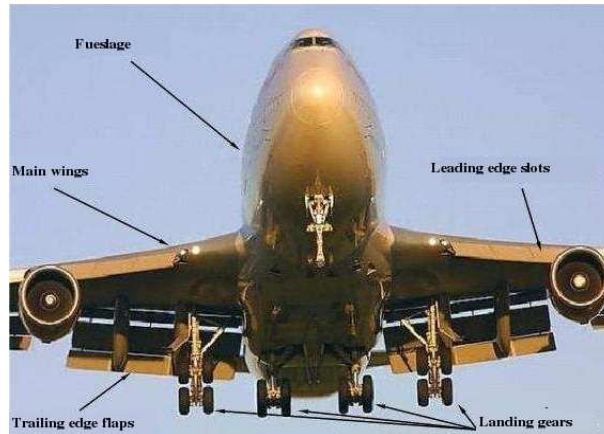


Figure 1 - Typical airframe cavities. (Picture courtesy Ben Pritchard, airliners.com)

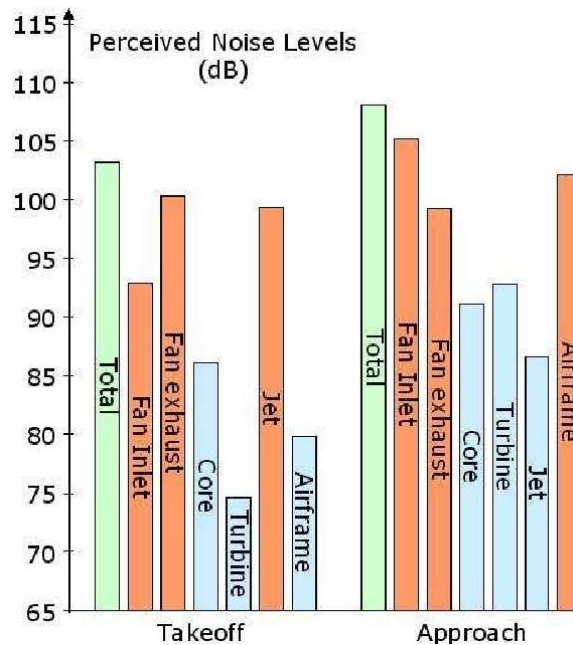


Figure 2 - Aircraft noise sources, during approach and takeoff Owens (1979).

cavity. Open cavities are characterised by the shear layer which attaches near the downstream corner, whereas closed cavities are characterised by the shear layer attachment at the bottom of the cavity and separation downstream. The basic difference can be summarised in figure 4. Open cavities are further divided into deep cavities and shallow cavities based on the aspect ratio $\frac{L}{D}$. Deep cavities are characterised by an aspect ratio $\frac{L}{D} < 1$, and shallow cavities by aspect ratio $\frac{L}{D} > 1$. Many of the airframe structures shown in figure 1 can be treated as a shallow open cavity. The main interest of this work is then to study these flows and to reduce the noise due to the acoustics.

There has also been numerous attempt to reduce the noise emitted from a cavity, by many heuristic

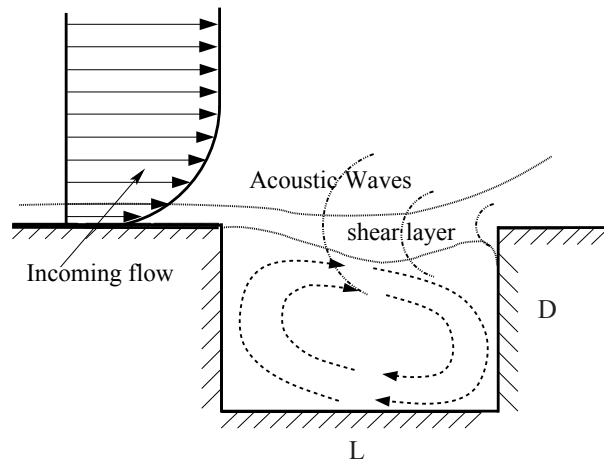


Figure 3 - A typical cavity flow.

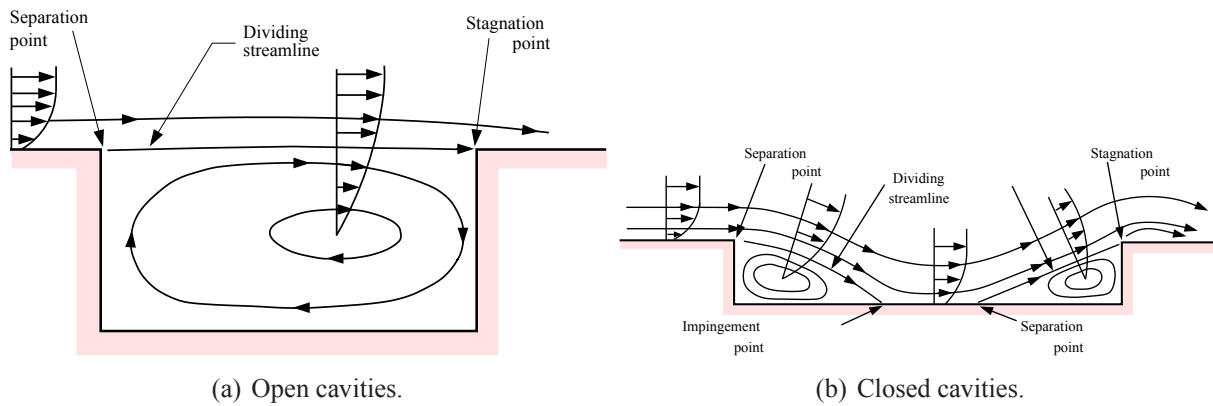


Figure 4 - Schematic representation of open and closed cavities.

means such as modifying the geometry by means of castellations, spoilers at the upstream edge of the cavity, so as to change the turbulent scales and hence reduce acoustic emissions. Use of synthetic jets delays the re-attachment of the shear layer and has been used in many experiments. With the advent of high performance computing as well as advanced experimental techniques such as the Particle Image Velocimetry (PIV), Laser Doppler Velocimetry (LDV) deep insights into the physics of cavity flows can be explored, with an aim to reduce the noise.

The traditional approaches like Direct Numerical Simulation (DNS) involve fully resolving the equations governing the flow dynamics *i.e.* the Navier-Stokes' equations down to the finest scale. Although this approach seems attractive it has inherent difficulties like the computational resources. An approach to reduce the computational time is the utilisation of Large Eddy Simulation (LES) where the major structures governing the flow (large eddies as they are called) are resolved and the finer scales are modelled. This approach also poses difficulties, particularly when used as an iterative tool for flow control, due to their high dimensional nature. The next proposition to reduce the dimensionality of the problem is by restricting our interest to the "most essential structures" which governs

the dynamics. The basic observation of fluid flow as a cascading phenomenon gives us the hint of this "essential" structures in terms of the energy, to obtain a low dimensional space. The reduced order model is then constructed as a projection of the high dimensional dynamics onto this lower dimensional subspace as summarised in figure 5.

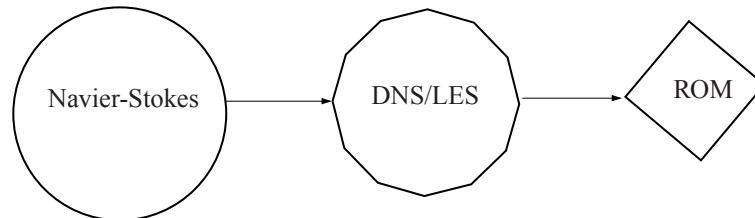


Figure 5 - Philosophy of reduced order modelling.

The aim of this thesis is to construct reduced order models for the cavity flows. The basic idea is to retain the most essential features of the flow called Proper Orthogonal Decomposition (POD) modes, which contain the maximum amount of information about the flow dynamics. By performing a DNS of the compressible Navier-Stokes equations to compute the flow of a large cavity, the POD modes are extracted. The Reduced Order Model (ROM) is then obtained by projecting the governing equation of fluid flow i.e the Navier Stokes equations on the subspace spanned the POD modes. This results in one having to solve a system of Ordinary Differential Equations (ODE) rather than the complicated system of Partial Differential Equations (PDE) and hence the name reduced order modelling. The well developed control theory is applied on this system of ODE's to obtain the noise reduction. Apart from being used in-lieu of the high fidelity model for control studies, the reduced order model obtained can also be used as a predictive tool to save computational resources. The overall strategy of using a reduced order model (ROM) can be summarised as shown in the figure 6.

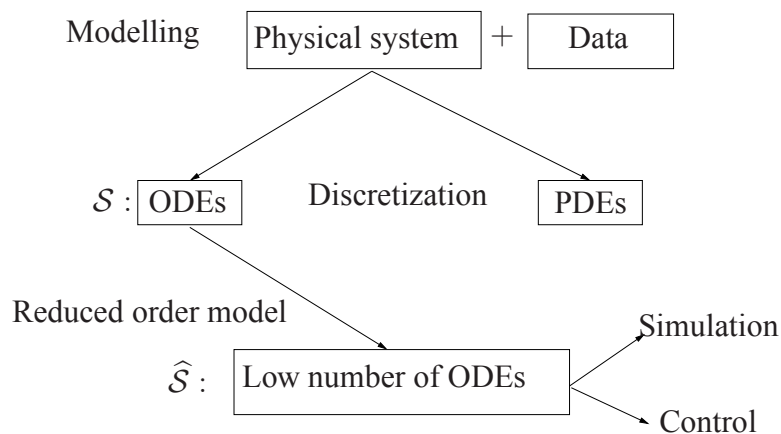


Figure 6 - A Schematic representation of Reduced Order Modelling.

Flow past an open cavity has been studied using ROM by [Rowley et al. \(2003\)](#) and [Gloerfelt \(2008\)](#) but without any application to flow control. More recently, ROM for controlled configurations has

been proposed by [Kasnakoğlu \(2007\)](#). In [Samimy *et al.* \(2007\)](#) the ROM for flows issued from an experiment has been used to design a controller. The major hurdle in using the ROM for control applications is the accuracy of the model in predicting the dynamics of the system even for short periods. Also difficulty arises when the control parameters are changed as in a real time simulation. Various numerical strategies termed as calibration techniques has been developed in the recent past to treat this problem as found in [Cordier *et al.* \(2009\)](#). The major contribution of this thesis is then to complete the full development as applied to cavities, like building up the ROM, including the effect of control, calibrating the model and finally performing control studies.

The outcome of the interest in reducing the cavity noise has resulted in the frame work of Aero-TraNet (Aerodynamic Training Network) projected which was a collaboration of 4 academic partners in Europe. The academic partners which included University of Leicester (U.K.), the Università degli Studi Roma Tre (Rome, Italy), Politecnico di Torino (Turin, Italy) and Institut de Mécanique des Fluides de Toulouse (Toulouse, France) were interested in various aspect of the cavity flow, like, numerical, experimental and flow control. This thesis was done in collaboration with LEA Poitiers, P. Comte for the DNS and L. Cordier for reduced order modelling. The thesis can be summarized as follows.

Organisation of the thesis

In chapter 1 we give a brief description of the numerical tool, namely the DNS used in this study and present some validation results. In chapter 2 the basic tools from control theory are introduced.

Chapter 3 concerns the basic theory of the technique of POD based ROM. The various techniques to include the effect of actuation in the ROM are summarized, with an application to the cavity flow.

In Chapter 4 the various definitions of errors between the calibrated dynamics and the original temporal dynamics are introduced and the different methods of calibration summarized are applied to the cavity flows. The methods are compared for accuracy. The calibration of the ROM is performed using a Tikhonov based regularization to obtain an accurate representation of the dynamics. We also present an improvement of the technique by introducing various type of weight matrix used in the definition of error. In the first method, we use a sensitivity analysis of the ROM, to determine the weights of the relevant terms which needs to be calibrated. The second approach is to use the energy content of the POD representation in forming the weight matrix to represent the errors.

In Chapter 5 a feedback control law based on the estimation of the observer dynamics has been presented. The observer matrix is constructed using a linear stochastic estimation. A sensitivity study of the actuated dynamics has been performed to determine the relevant terms in the linearisation of the model. Finally an Linear Quadratic Gaussian (LQG) controller is designed to obtain an optimal solution, which is introduced in the Direct Numerical Simulation to obtain a decrease in spectra of the cavity acoustic mode.

Chapter 1

Description and validation of the numerical tool

Description et validation de l'outil numérique

Dans cette partie, les outils numériques utilisés pour les études de modèle réduit et du contrôle sont décrits. Le jet synthétique est introduit pour contrôler les instabilités de cavité. L'écoulement de cavité est largement étudiée dans la littérature. Il présente des instabilités auto-entretenues qui sont difficiles à prédire numériquement (sensibilité aux différents paramètres numériques). La cavité est aussi le siège d'interactions aéroacoustiques qui nécessitent un schéma numérique d'ordre supérieur et peu dissipatif pour capter les ondes acoustiques. Le code NIGLO utilisé est développé par Pierre Comte de l'Université de Poitiers. Il est capable de résoudre les équations de Navier Stokes compressibles en instationnaire et en tridimensionnel. La discrétisation différences finies de quatrième ordre est faite sous forme conservative.

Paramètres de non-dimensionalisation

Le code résout les équations sous forme adimensionnelle. L'adimensionalisation dépend fortement des échelles caractéristiques pour rendre les variables adimensionnelles. La forme adimensionnelle des équations de Navier-Stokes incorpore trois nombres adimensionnel, les nombres de Reynolds, de Mach et de Prandtl.

Equations du mouvement en coordonnées cartésiennes

Les équations de Navier Stokes compressibles sont écrites sous forme conservatives. Il s'agit des équations de continuité, de conservation de la quantité de mouvement et de l'énergie. Le tenseur des contraintes de cisaillement est exprimé sous l'hypothèse de Newton-Stokes et le flux thermique est donné à l'aide de la loi de Fourier. La viscosité en fonction de la température est exprimée avec la loi de en puissance.

Avancement en temps

Le schéma temporel utilisé est un schéma explicite aux différences finies utilisant la procédure prédicteur-correcteur. Une différenciation décentrée conservative est utilisée pour les deux pas temporels du schéma en alternant la direction de discrétisation entre le pas prédicteur et correcteur. Il en résulte globalement un schéma spatial centré de quatrième ordre pour les termes d'advection et de second ordre pour ceux de la diffusion. La discrétisation temporelle est du second ordre.

Conditions aux limites

Pour les parois, la condition d'adhérence est appliquée. La forme simplifiée de l'équation dynamique reliant la pression et le tenseur de cisaillement est aussi utilisée. Pour l'état thermodynamique on définit soit une paroi adiabatique ou soit une paroi isotherme.

Conditions aux limites non-réfléchissantes

Pour éviter toute réflexion sur les limites du domaine de calcul, deux types de conditions peuvent être adoptées: des conditions physiques dictées par le problème continu initial ou des conditions numériques nécessaires à la méthode discrète pour compléter l'ensemble des conditions physiques. Les conditions aux limites basées sur les caractéristiques (NSCBC) de [Poinsot & Lele \(1992\)](#) est une méthode pour spécifier à la fois les conditions physiques et numériques pour les équations d'Euler et pour celles de Navier Stokes. La méthode NSCBC est basée sur une analyse monodimensionnelle locale en non-visqueux (LODI) des ondes traversant les limites du domaine. Les amplitudes des ondes caractéristiques associées à chaque vitesse caractéristique sont données (équations 1.19 à 1.21). On distingue les conditions aux limites non-réfléchissantes pour une entrée subsonique (équations 1.22 à 1.27) de celles pour une sortie subsonique (équations 1.28 et 1.29).

Validation du code numérique pour le cas de la cavité

On présente les résultats pour une cavité de rapport d'aspect $L/D = 2$. L'écoulement est initialisé par une couche limite laminaire pour avoir une épaisseur $\delta/D = 0.28$ au coin amont de la cavité. Le nombre de Reynolds basé sur la profondeur de la cavité est de 1500 et le nombre de Mach est de 0.6. Le domaine de calcul a une longueur de $14D$ et une hauteur de $7D$ (figure 1.1). Le tableau 1.1 donne la taille des différents maillages utilisés. Le maillage choisi est donné sur la figure 1.2 et correspond au maillage M. La figure 1.4 montre les niveaux de pression sonore (SPL) pour le champ acoustique au-dessus de la cavité et le spectre de vitesse normal en un point de la couche cisailée. Le niveau de pression sonore maximal est de 170 dB qui est inférieur à celui obtenu par [Rowley et al. \(2002\)](#) (180 dB). Ceci peut s'expliquer par la différence de précision des schémas (4^{ème} ici et 6^{ème} pour eux). Les niveaux SPL sont cependant en accord avec les résultats expérimentaux de [Krishnamurthi \(1956\)](#) (168 dB). Le spectre montre la valeur typique correspondant au second mode de Rossiter (avec deux tourbillons en moyenne entre les deux coins de la cavité). Les oscillations auto-entretenues sont quasi-périodiques, avec un spectre présentant une fréquence dominante.

Introduction au contrôle

Le contrôle de la cavité résonante est réalisé à l'aide d'un jet synthétique en modifiant la condition au limite convenablement. Le contrôle par jet synthétique a été réalisé auparavant numériquement et expérimentalement. L'objectif du contrôle est de dévier la couche cisailée pour qu'elle n'impacte pas sur le coin aval et éviter le phénomène du retour (feedback). Comme on peut le voir sur la figure 1.6, sous l'effet du jet, la couche cisailée peut impacter totalement, partiellement ou pas du tout. Plusieurs positions ont été testées avant le coin amont pour améliorer l'efficacité. Ceci peut être fait en mesurant la sensibilité de l'écoulement au coin amont. Il a été montré que c'est le point le plus sensible aux perturbations externes. Le forçage est typiquement de la forme $A \sin(\omega t)$ et l'actionneur est introduit juste avant le coin de cavité ($x \in [-0.15; -0.05]$ et $y = 0$). Le spectre de vitesse pour un forçage de la forme $A \sin(\omega t)$ (figure 1.7) conduisant à la diminution du mode de Rossiter. Il y a une redistribution de l'énergie sur d'autres pics. L'actionnement est cependant non optimal. Un des objectifs de ce travail est de déterminer la fréquence et l'amplitude optimales en utilisant le contrôle dans le modèle d'ordre réduit.

Conclusion

Dans ce chapitre nous avons introduit l'outil numérique, les équations, la discrétisation et les conditions aux limites utilisées. Le code a été validé sur le cas de la cavité. L'introduction du contrôle avec un jet synthétique placé avant le coin amont est décrite. On note la diminution du mode de Rossiter et la distribution de l'énergie sur d'autres pics. Les outils pour réaliser un contrôle optimal seront décrits dans la suite.

1.1 Introduction

In this chapter the basic numerical tool used in this work is described. We perform a DNS resolving of a 2D cavity flow. Regarding the introduction of actuation a synthetic jet is introduced at the upstream boundary to control the instabilities. There has been a large body of literature on physics of the cavity flow as can be found in [Rowley *et al.* \(2002\)](#), [Larchevêque *et al.* \(2004\)](#), [Bres & Colonius \(2008\)](#), [Rowley & Williams \(2006\)](#). Flows with self sustained oscillations are difficult to model as they are very sensitive to the disturbances, due to shear layer amplification. Even a small error in the numerical discretisation at the cavity leading edge can result in a large amplification of the errors downstream of the cavity. Problems can also arise due to the artificial reflections at the computational boundary, and may sometimes be indistinguishable from the physical disturbances, causing the appearance of non-physical frequencies. Also in the case of cavity flows the feedback mechanism is acoustic and of many orders smaller than the hydrodynamic disturbances, which necessitates the utilisation of a high order, low-dissipative numerical method to resolve them. The code NIGLO used in this study is capable of solving three dimensional unsteady compressible Navier-Stokes equations on multi-block curvilinear grid. The discretisation is through a fourth order finite difference scheme for the advective fluxes and second order scheme for the diffusive fluxes. The temporal discretisation is second order accurate. The code was initially developed by Professor Pierre Comte at the University of Poitiers.

1.2 Non-dimensionalisation parameters

Non-dimensionalising the flow-field parameters removes the necessity of converting from one system to another within the code. The process of non-dimensionalisation depends on the choice of the parameter for the problem. In the code all the parameters of the simulation are non-dimensionalised by the reference values, which are the characteristics of the flow namely the Reynolds number, Mach number & Prandtl number. The Reynolds number is used to quantify the convective effects to the viscous effects, whereas Mach number gives the ratio between the reference velocity and the speed of the sound, finally the Prandtl number gives the ratio between the heat transfer by viscous diffusion and heat transfer by thermal conduction.

$$\begin{aligned}x^* &= \frac{x}{L_0} & y^* &= \frac{y}{L_0} & z^* &= \frac{z}{L_0} & u^* &= \frac{u}{U_0} & v^* &= \frac{v}{U_0} \\w^* &= \frac{w}{L_0} & P^* &= \frac{P}{P_0} & \rho^* &= \frac{\rho}{\rho_0} & T^* &= \frac{T}{T_0} & t^* &= \frac{U_0 t}{L_0}\end{aligned}$$

Where all the quantities with (*) are the non-dimensionalised scales used in the code, and values with (0) are reference values of the flow-field. In the following we use only non dimensional variables without *

1.3 Governing equations in cartesian coordinate system

The fully compressible Navier-Stokes equation in a conservative form can be written for the non dimensionalised variables as

$$\frac{\partial U}{\partial t} - \text{div} \mathcal{F} = 0 \quad (1.1)$$

with $\mathcal{F} = (E, F, G)$ and $U = (\rho, \rho u, \rho v, \rho w, \rho e)$.

In Cartesian coordinates we have,

$$\frac{\partial U}{\partial t} + \frac{\partial E}{\partial x} + \frac{\partial F}{\partial y} + \frac{\partial G}{\partial z} = 0 \quad (1.2)$$

where E, F, G are the non-dimensionalised fluxes defined by:

$$E = \begin{bmatrix} -\rho u^2 - \frac{1}{\gamma M^2} p + \frac{\mu}{Re} \tau_{xx} \\ -\rho uv + \frac{\mu}{Re} \tau_{xy} \\ -\rho uw + \frac{\mu}{Re} \tau_{xz} \\ -u(\rho e + p) + \gamma M^2 \frac{\mu}{Re} (u\tau_{xx} + v\tau_{xy} + w\tau_{xz}) + \frac{\gamma}{\gamma - 1} \frac{\mu}{Re Pr} q_x \end{bmatrix}$$

$$F = \begin{bmatrix} -\rho uv - \frac{1}{\gamma M^2} p + \frac{\mu}{Re} \tau_{xy} \\ -\rho v^2 - \frac{1}{\gamma M^2} p + \frac{\mu}{Re} \tau_{yy} \\ -\rho vw + \frac{\mu}{Re} \tau_{yz} \\ -v(\rho e + P) + \gamma M^2 \frac{\mu}{Re} (u\tau_{xy} + v\tau_{yy} + w\tau_{yz}) + \frac{\gamma}{\gamma - 1} \frac{\mu}{Re Pr} q_y \end{bmatrix}$$

$$G = \begin{bmatrix} -\rho uw - \frac{1}{\gamma M^2} p + \frac{\mu}{Re} \tau_{xz} \\ -\rho vw + \frac{\mu}{Re} \tau_{yz} \\ -\rho w^2 - \frac{1}{\gamma M^2} p + \frac{\mu}{Re} \tau_{zz} \\ -w(\rho e + p) + \gamma M^2 \frac{\mu}{Re} (u\tau_{xz} + v\tau_{yz} + w\tau_{zz}) + \frac{\gamma}{\gamma - 1} \frac{\mu}{Re Pr} q_z \end{bmatrix}$$

The Reynolds number is based on the characteristic length L_0 of the cavity, and velocity U_0 , which represents the characteristics of the flow can be defined by:

$$Re = \frac{\rho_0 U_0 L_0}{\mu_0} \quad (1.3)$$

1. Description and validation of the numerical tool

With μ_0 is the dynamic viscosity calculated at the same point of reference chosen for the velocity U_0 and for the density ρ_0 . In the same manner, the Mach number based on a reference temperature T_0

$$M = \frac{U_0}{\sqrt{R\gamma T_0}} \quad (1.4)$$

The Prandtl number which corresponds to the ratio of the kinematic viscosity and thermal diffusivities:

$$Pr = \frac{\mu_0 C_p}{\lambda_0} \quad (1.5)$$

The total energy E is given by the equation of state as:

$$\rho E = \frac{1}{\gamma - 1} p + \frac{\gamma M^2}{2} \rho (u^2 + v^2 + w^2) \quad (1.6)$$

With the Stokes hypothesis the viscous stress tensor is proportional to the trace free part of the strain rate tensor.

$$\tau_{ij} = \left(\frac{\partial u_i}{\partial x_j} + \frac{\partial u_j}{\partial x_i} - \frac{2}{3} \frac{\partial u_l}{\partial x_l} \delta_{ij} \right) \quad (1.7)$$

With the above non-dimensionalisation, the Fourier law reads as

$$q_i = -k \frac{\partial T}{\partial x_i} \quad (1.8)$$

For taking into account the variation of dynamic viscosity with temperature a power law has been used and is given by

$$\mu(T) = \left\{ \mu(T_0) \left(\frac{T}{T_0} \right)^{0.7} \right. \quad (1.9)$$

1.4 Time advancement

The time advancement scheme employed in NIGLO is an explicit finite difference scheme of predictor-corrector type as proposed by [Gottlieb & Turkel \(1975\)](#). Conservative decentered differencing is utilised for two steps of time advancement scheme which alters the discretisation between the predictor and corrector steps, resulting in a globally centered scheme which is 4th order for the advection term and 2nd order for the diffusion term in space respectively. The discretisation is given by

Predictor step:

$$U_i^{n+1/2} = U_i^n + \left(\begin{array}{l} \frac{\Delta t}{\Delta x} \left[-\frac{7}{6} E_i^n + \frac{8}{6} E_{i+1}^n - \frac{1}{6} E_{i+2}^n \right] \\ \frac{\Delta t}{\Delta y} \left[-\frac{7}{6} F_i^n + \frac{8}{6} F_{i+1}^n - \frac{1}{6} F_{i+2}^n \right] \\ \frac{\Delta t}{\Delta z} \left[-\frac{7}{6} G_i^n + \frac{8}{6} G_{i+1}^n - \frac{1}{6} G_{i+2}^n \right] \end{array} \right) \quad (1.10)$$

Corrector step:

$$U_i^{n+1} = \frac{1}{2}(U_i^{n+1/2} + U_i^n) + \begin{pmatrix} \frac{\Delta t}{\Delta x} \left[\frac{7}{12} E_i^{n+1/2} + \frac{8}{12} E_{i+1}^{n+1/2} - \frac{1}{12} E_{i+2}^{n+1/2} \right] \\ \frac{\Delta t}{\Delta y} \left[\frac{7}{12} F_i^{n+1/2} + \frac{8}{12} F_{i+1}^{n+1/2} - \frac{1}{12} F_{i+2}^{n+1/2} \right] \\ \frac{\Delta t}{\Delta z} \left[-\frac{7}{6} G_i^{n+1/2} + \frac{8}{12} G_{i+1}^{n+1/2} - \frac{1}{12} G_{i+2}^{n+1/2} \right] \end{pmatrix} \quad (1.11)$$

The predictor-corrector scheme described above is valid for uniform mesh. In our case when we use mesh refinement to resolve the boundary layer, corners of cavity the mesh spacing is not constant. In that case we use a transformation of the physical variables into a new coordinates of constant length and perform the discretisation. The derivatives are then transformed back onto the physical coordinates by the inverse transform.

1.5 Boundary conditions

1.5.1 Wall boundary condition

No slip condition at the wall is applied, so that all the velocity components at the wall are zero *i.e.*

$$\begin{aligned} u_{\text{wall}} &= 0 \\ v_{\text{wall}} &= 0 \\ w_{\text{wall}} &= 0 \end{aligned} \quad (1.12)$$

The conservation of momentum equation is reduced to the following form

$$-\frac{1}{\gamma M^2} \frac{\partial p}{\partial x_n} + \left(\frac{\mu}{Re} \right) \left(\frac{\partial \tau_{ij}}{\partial x_j} \right) = 0 \quad (1.13)$$

It only remains to determine the thermodynamic state at the wall, which is chosen as isothermal for the case of the cavity flow.

1.5.2 Non-reflective boundary conditions

The accuracy of unsteady flow calculations relies on accurate treatment of boundary conditions. Due to the limit of computational resource, usually only a limited computational domain is considered for an unsteady flow calculations. This means that we have to "cut off" the domain that is not of our primary interest. However, the cut boundaries may cause artificial wave reflections which may include both physical and numerical waves. Such waves may bounce back and forth within the computational domain and may seriously contaminate the solutions.

Two types of conditions have to be provided to solve numerically the fully compressible Euler or Navier-Stokes equations

1. Description and validation of the numerical tool

- Physical conditions which are the boundary conditions dictated by the original non-discretised problem.
- Soft conditions which are numerical conditions required by the discrete method to complete the set of physical conditions.

As described in [Poinsot & Lele \(1992\)](#), the Navier-Stokes characteristic boundary condition (NSCBC) specifies both the physical and soft boundary conditions for Euler and for Navier-Stokes equations. In this method physical conditions are specified according to the well-posedness of Navier-Stokes equation.

Viscous condition for Navier-Stokes are added to the inviscid Euler equations to obtain the right number of boundary conditions for Navier-Stokes. The viscous conditions are used only to compute the viscous terms in the conservation equations at the boundary and, therefore are not strictly enforced. The method relaxes smoothly to the Euler boundary condition when the viscosity goes to zero.

Soft conditions are constructed without any extrapolation. The NSCBC method is based on a local one dimensional inviscid (termed LODI) analysis of the waves crossing the boundary. The amplitude variation of the waves entering the domain are estimated from an analysis of the local one dimensional inviscid equations. To explain further consider the quasi-linear form of the Euler equation

$$\frac{\partial V}{\partial t} + A \frac{\partial V}{\partial x} + B \frac{\partial V}{\partial y} + C \frac{\partial V}{\partial z} = 0 \quad (1.14)$$

Which can also be written in the following compact form:

$$\frac{\partial V}{\partial t} + (\vec{A} \cdot \vec{\nabla}) V = 0 \quad (1.15)$$

Where $V = (u, v, w, T, p)^t$ is the vector of primitive variables and the matrices A, B, C are defined as:

$$A = \begin{bmatrix} u & \rho & 0 & 0 & 0 \\ 0 & u & 0 & 0 & 1/\rho \\ 0 & 0 & u & 0 & 0 \\ 0 & 0 & 0 & u & 0 \\ 0 & \gamma p & 0 & 0 & u \end{bmatrix} \quad B = \begin{bmatrix} v & 0 & \rho & 0 & 0 \\ 0 & v & 0 & 0 & 0 \\ 0 & 0 & v & 0 & 1/\rho \\ 0 & 0 & 0 & v & 0 \\ 0 & 0 & \gamma p & 0 & v \end{bmatrix} \quad C = \begin{bmatrix} w & 0 & 0 & \rho & 0 \\ 0 & w & 0 & 0 & 0 \\ 0 & 0 & w & 0 & 0 \\ 0 & 0 & 0 & w & 1/\rho \\ 0 & 0 & 0 & \gamma p & w \end{bmatrix}$$

In our case, we are interested in the propagation of the vector V normal to the boundary. So we introduce the matrix E_n such that

$$E_n = A n_x + B n_y + C n_z \quad (1.16)$$

or

$$E_n = \vec{A} \cdot \vec{n} \quad (1.17)$$

where $n = (n_x, n_y, n_z)^t$ is the unit normal. The matrix of the eigenvalues obtained by diagonalizing E_n is

$$\lambda_n = L_n E_n L_n^{-1} n = \text{diag}(\lambda_1, \lambda_2, \lambda_3, \lambda_4, \lambda_5) = \text{diag}(u_1 - c, u_1, u_1, u_1, u_1 + c) \quad (1.18)$$

Here c is the speed of sound. The amplitudes of the characteristics waves L'_i s associated with each characteristic velocity are given by:

$$\begin{aligned} L_1 &= \lambda_1 \left(\frac{\partial p}{\partial x_1} - \rho c \frac{\partial u_1}{\partial x_1} \right) \\ L_2 &= \lambda_2 \left(c^2 \frac{\partial \rho}{\partial x_1} - \frac{\partial p}{\partial x_1} \right) \\ L_3 &= \lambda_3 \frac{\partial u_2}{\partial x_1} \\ L_4 &= \lambda_4 \frac{\partial u_3}{\partial x_1} \\ L_5 &= \lambda_5 \left(\frac{\partial p}{\partial x_1} + \rho c \frac{\partial u_1}{\partial x_1} \right) \end{aligned} \quad (1.19)$$

The LODI system can be cast in many different forms depending on the choice of variables. In terms of the primitive variable, this system can be written as

$$\begin{aligned} \frac{\partial \rho}{\partial t} + \frac{1}{c^2} [L_2 + \frac{1}{2}(L_5 + L_1)] &= 0 \\ \frac{\partial p}{\partial t} + \frac{1}{2}(L_5 + L_1) &= 0 \\ \frac{\partial u_1}{\partial t} + \frac{1}{2\rho c}(L_5 - L_1) &= 0 \\ \frac{\partial u_2}{\partial t} + L_3 &= 0 \\ \frac{\partial u_3}{\partial t} + L_4 &= 0 \end{aligned} \quad (1.20)$$

The LODI relations are used to obtain the relations on the L'_i s which will be used later in the system of conservation equation. Using the LODI relation alone may also provide a simple but approximate method to derive boundary conditions. For example assuming non-reflection at the outlet is equivalent to imposing $L_1 = 0$.

$$\frac{\partial p}{\partial t} - \rho c \frac{\partial u_1}{\partial t} = 0 \quad (1.21)$$

1.5.3 Subsonic infow boundary condition

For the case of infow we consider the case where all components of velocity u_1 , u_2 , and u_3 as well as the temperature T are imposed. At the inlet u_1 is imposed, the LODI relation suggest the following

expression for L_5 :

$$L_5 = L_1 - 2\rho c \frac{\partial U}{\partial t} \quad (1.22)$$

$$L_2 = \frac{1}{2}(\gamma - 1)(L_5 + L_1) + \frac{\rho c^2}{T} \frac{dT}{dt} \quad (1.23)$$

Also we have

$$L_3 = -\frac{\partial V}{\partial t} \quad (1.24)$$

and

$$L_4 = -\frac{\partial W}{\partial t} \quad (1.25)$$

The density can now be obtained by using the equation

$$\frac{\partial \rho}{\partial t} + d_1 = 0 \quad (1.26)$$

Where d_1 is given by

$$d_1 = \frac{1}{c^2} [L_2 + \frac{1}{2}(\gamma - 1)(L_5 + L_1)] \quad (1.27)$$

In this case L_1 is computed using the interior points from (1.19).

1.5.4 Subsonic non-reflecting outflow boundary condition

For subsonic flow at exit, the eigenvalue $\lambda_1 = u - c$ is negative and the disturbance propagates into the domain from outside. L_2 to L_5 can be still calculated from the interior points. However, L_1 corresponding to the eigenvalue of $u - c$ must be treated differently. The conventional method to provide a well posed boundary condition is to impose $p = p_\infty$ at the outflow boundary.

This treatment however will create acoustic wave reflections, which may be diffused and eventually disappear at the steady state. In case of unsteady flows, the wave reflection may contaminate the flow solutions. To avoid wave reflections, the following soft boundary condition as suggested by [Poinsot & Lele \(1992\)](#) is used.

$$L_1 = K(p - p_\infty) \quad (1.28)$$

where K is a constant and is determined by

$$K = \sigma(1 - M^2)c/L \quad (1.29)$$

M is the maximum Mach number in the flow, L is a characteristic size of the domain, and σ is a constant. The preferred range for constant σ is 0.2 – 0.5. When $\sigma = 0$ (1.29) imposes the amplitude of reflected waves to 0 as suggested by [Thompson \(1987\)](#) and termed as "perfectly non-reflecting". In this study we choose the value of $\sigma = 0.25$.

1.6 Modelling cavity flows using NIGLO

In this section we present the results of validation for the cavity of L_e/D ratio of 2. The flow is initialised by a laminar boundary layer so as to have a thickness of $\delta/D = 0.28$ at the leading edge of the cavity. The Reynolds number of the flow based on the cavity depth is 1500 and the flow Mach number is 0.6 as in [Rowley et al. \(2002\)](#). The representative flow in our case is laminar due to the restriction of computational resources for a real time turbulent simulations. Also it is worthwhile to use scale down the problem to laminar regions to test the basic developments. The computational domain consists of $14D$ in the stream-wise direction and $7D$ in the vertical direction. The cavity flow configuration is as shown in figure 1.1. For the mesh a double hyperbolic tangent distribution is used in both the stream-wise and vertical directions, with a stretch ratio of 5%. The influence of mesh

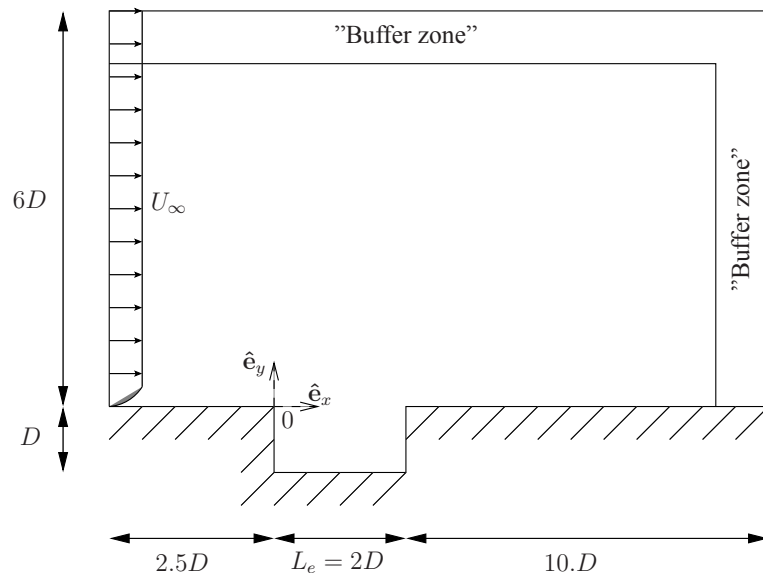


Figure 1.1 - Schematic diagram of cavity configuration and computational domain.

resolution on numerical results is measured by performing a mesh convergence studies to obtain grid independent results. The different mesh sizes used in the studies is given in table 1.1. The typical mesh used in this study is shown in figure 1.2 and corresponds to mesh M.

Figure 1.3 shows the instantaneous contours of vorticity, the size of the recirculation zone being the same order as the depth. Figure 1.4(a) shows the overall sound pressure level (SPL) for the acoustic field above the cavity. The maximum SPL is about 170 dB at a point near the downstream edge.

This is lower than the value reported in [Rowley et al. \(2002\)](#) where a value of 180 dB is reported. This may be due to the artifact of the numerical scheme used in computation which is 4^{th} order accurate in the present study whereas it is 6^{th} order accurate in the case of [Rowley et al. \(2002\)](#). The SPL levels is however in agreement with the experimental results of [Krishnamurthi \(1956\)](#) where a typical value of around 168 dB is reported.

1. Description and validation of the numerical tool

Mesh Type	Block 1	Block 2 (cavity)	CFL
Coarse (C)	185 × 80	60 × 40	0.75
Medium (M)	260 × 80	102 × 80	0.6
Fine (F)	335 × 108	120 × 100	0.6

Table 1.1 - Mesh sizes used in computation.

The spectra corresponding to the normal component of velocity at a point in the shear layer is shown in Figure 1.4(b) and shows a single frequency. The value of Strouhal number is $St_2 = \frac{f_2 L}{U_\infty} = 0.72$ in good agreement with the value of 0.74 determined by the Rossiter's formula [Delprat \(2006\)](#)

$$St = \frac{(n - 0.25)}{(M + 1/0.57)} \quad \text{for } n = 2$$

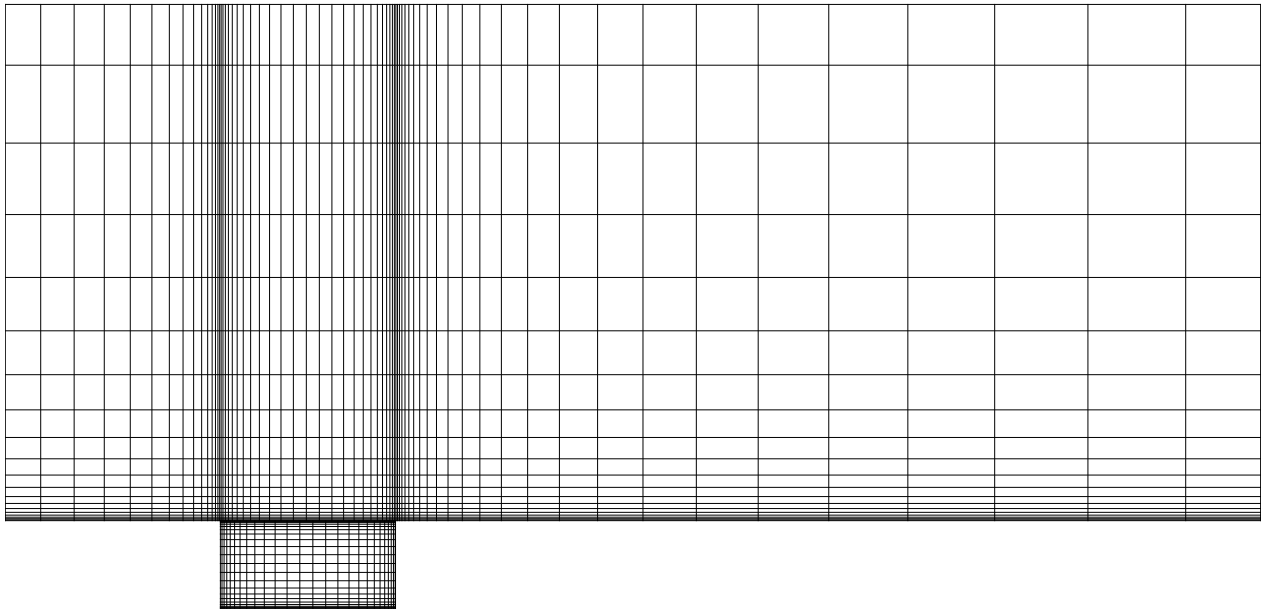


Figure 1.2 - Typical mesh used in cavity corresponding to M in table 1.1. One in every fourth cell is plotted.

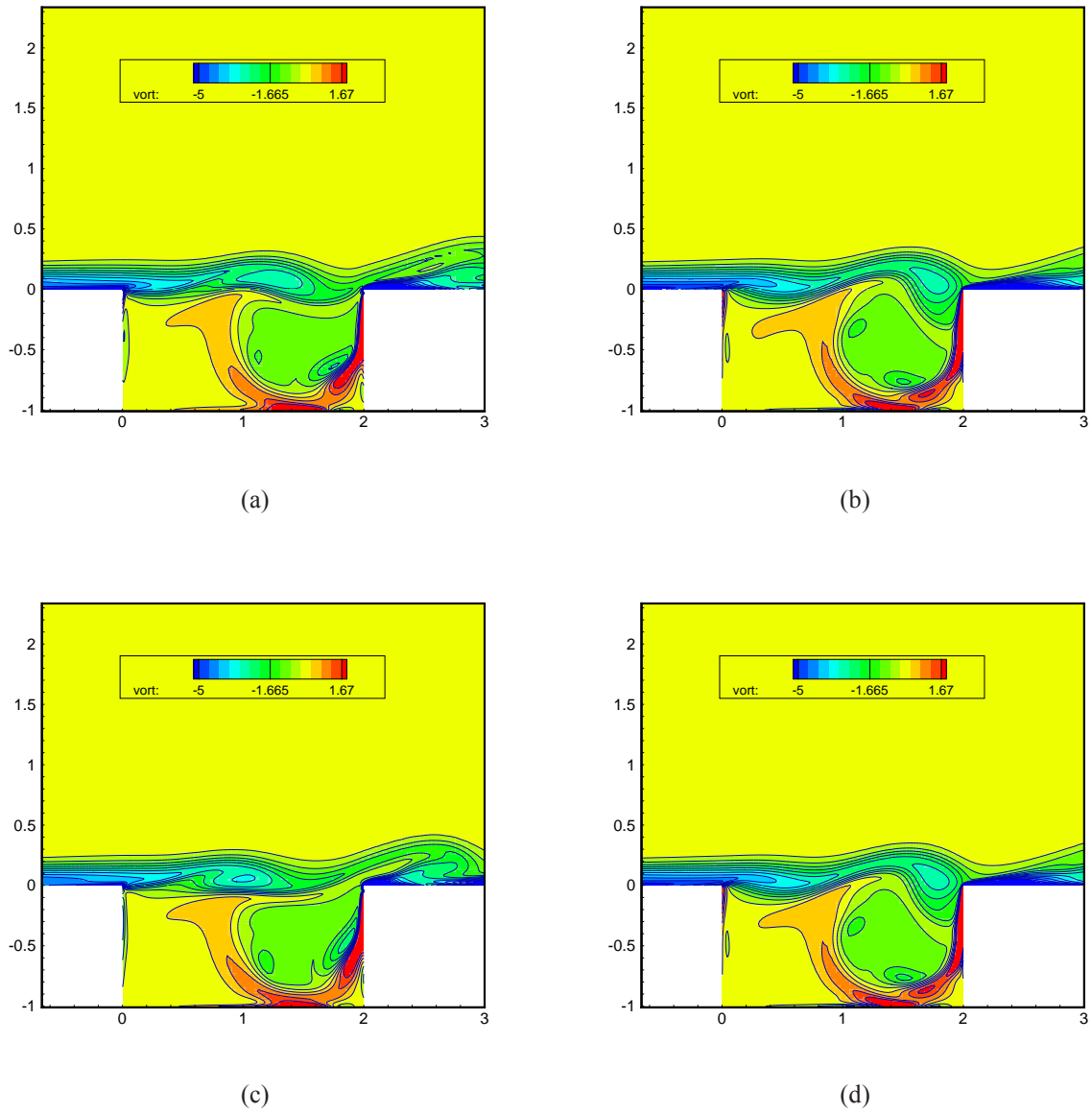
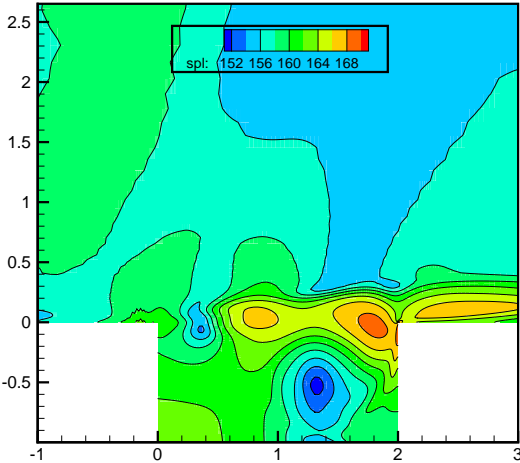
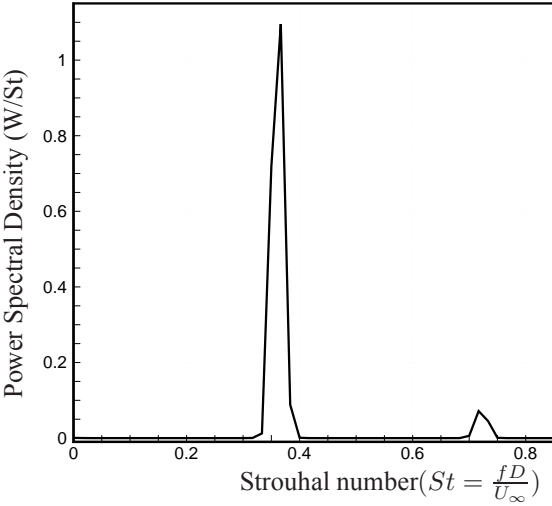


Figure 1.3 - Instantaneous snapshots of vorticity. 15 contours in the range $\frac{\omega D}{U} \in [-5, 1.67]$ are plotted. Only a small portion of the computational domain near the cavity is shown.

1. Description and validation of the numerical tool



(a) SPL



(b) Spectra

Figure 1.4 - SPL and spectra of the normal component of velocity at $y = 0$ and $x = 1.8D$ in the shear layer.

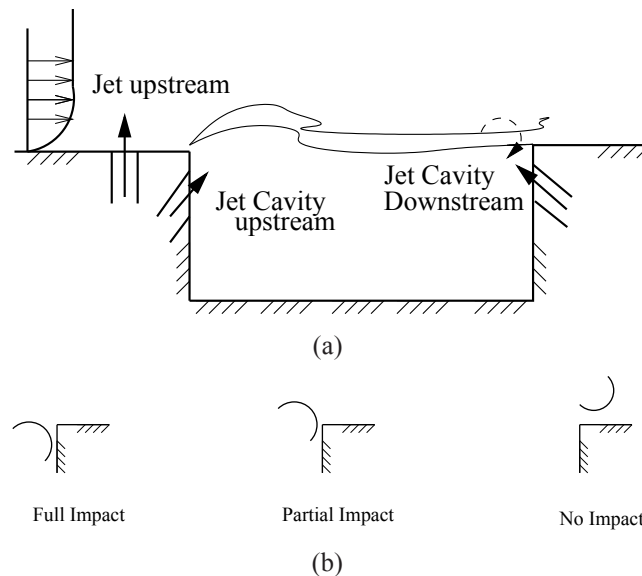


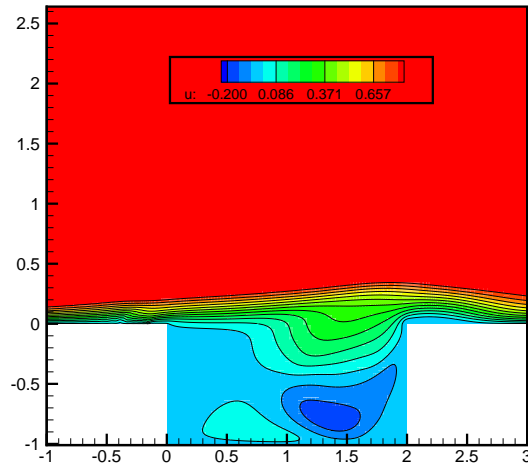
Figure 1.5 - Schematic representation of the action of jet and its effect on the impingement of the shear layer.

1.7 Introduction of control

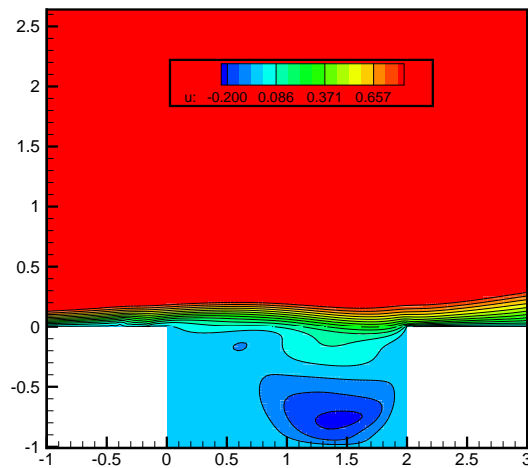
The control of the cavity is achieved by means of a synthetic jet, which is achieved by modifying the boundary condition in a suitable way. The introduction of control by means of the synthetic jet has been previously performed by [Shutian *et al.* \(2007\)](#) for the case of flow separation around an airfoil, [Kestens \(1999\)](#) and [Samimy *et al.* \(2007\)](#) for the case of the cavity. for the experimental control of cavity.

The basic physics behind the control of cavity resonance is to deflect the shear layer from impinging on the downstream edge of the cavity thereby arresting the feedback mechanism. As a result of the jet the shear layer can impinge on the downstream edge either fully, partially or can just pass over without any impingement as shown in figure 1.5. Different positions of the jet has been tried, and the position just before the upstream edge of the cavity proves to be more effective. This can be explained by measuring the sensitivity of the flow, where the upstream edge is more sensitive to external flow disturbances as shown in [Moret-Gabarro \(2009\)](#). The forcing is typically of the form $A \sin(\omega t)$, and the actuation is introduced just before the leading edge of the cavity ($x \in [-0.15; -0.05]$ and $y = 0$), the length of actuation is dependent on cost factors, such as the cost of the actuator in case of experiments or the computational cost in case of numerical simulation. The snapshots of the stream wise component of velocity is shown in figure 1.6, showing the case of no impact and partial impact of the shear layer on the trailing edge.

1. Description and validation of the numerical tool



(a) No impact of shear layer on the downstream edge.



(b) Partial impact of the shear layer on the downstream edge.

Figure 1.6 - *Instantaneous snapshots of the stream wise component of velocity depicting the effect of actuation. The forcing is introduced at $x \in [-0.15; -0.05]$ and $y = 0$ and is of the form $0.2 \sin(0.4t)$.*

The spectra for a typical forcing of the form $A \sin(\omega t)$ is shown in the figure 1.7, Here the peak

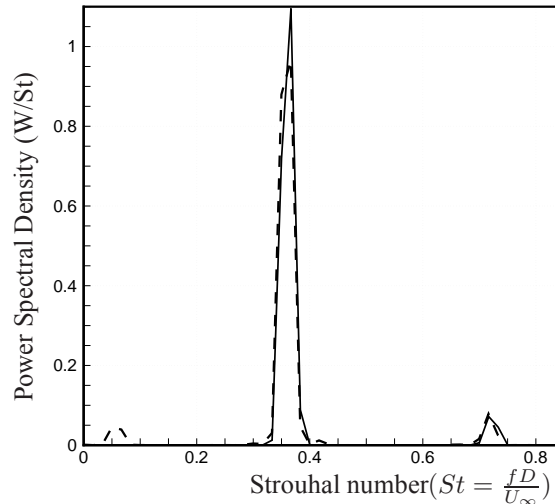


Figure 1.7 - Spectra at $y = 0$ and $x = 1.8D$ in the shear layer for the normal component of velocity for the actuated flow (dashed line). The forcing is of the form $0.2 \sin(0.4t)$. The spectra is compared for flow without any actuation (solid line).

corresponding to the Rossiter mode is reduced. One of the objects of the current work is to determine the optimal forcing frequency and amplitude by utilising a reduced order model and check its effect by introducing it in the DNS code.

1.8 Conclusion

In this chapter we have introduced the basic numerical tool used in this study with respect to the governing equations, numerical discretisation and the various boundary conditions used. The code has been validated for the cavity flow configuration and will be used through in this study. Introduction of control by means of a synthetic jet at the upstream edge of the cavity, where the flow is more sensitive to perturbations is performed. The associated spectra shows a decrease at the peak Rossiter mode followed by the appearance of new peaks suggesting the need for optimal criteria for injection. Various tools to perform the optimal control using ROM will be developed in the subsequent chapters.

Chapter 2

Basic tools from control theory

Introduction

Ce chapitre présente brièvement les différentes théories du contrôle actif [Bewley & Agarwal \(1996\)](#), [Bewley & Liu \(1998\)](#), [Kim & Bewley \(2007\)](#), [Bagheri et al. \(2009b\)](#) qui ont trouvé des applications en mécanique des fluides lors de ces 15 dernières années, et qui sont utilisées en partie dans ce travail. On qualifie en premier lieu le type de contrôle en fonction de la loi de contrôle et de son action. On parle de contrôle en boucle ouverte (open loop) lorsque la loi de contrôle est déterminée optimalement pour stabiliser un système initialement instable. La loi n'est pas modifiable au cours du processus de contrôle. A l'opposé, dans le contrôle en boucle fermée (close-loop), une loi de retour (feedback) lie le contrôle à l'état réel et réactualisé du système, assurant une stabilisation plus efficace.

Avant de chercher une loi de contrôle, on doit aussi regarder les aspects de contrôlabilité (ou commandabilité) et d'observabilité. La contrôlabilité qualifie la capacité du système à atteindre un état souhaité à partir d'une certaine loi de contrôle et d'une bonne condition initiale. La stabilisabilité, associée à la contrôlabilité, assure qu'il existe une loi de retour capable de stabiliser le système. Cela revient à dire que les modes non commandables sont tous stables. Enfin l'observabilité, qui mathématiquement est une notion duale à la notion de contrôlabilité, indique que l'observation des entrées et sorties du système, pendant un intervalle de temps fini, permet de retrouver l'état initial et donc l'état complet.

Contrôle des écoulements en boucle ouvert et optimisation sous contrainte

Un problème de contrôle est bien posé si on peut clairement définir :

- *la variable d'état du système ϕ .*
- *la variable de contrôle c .*

- une fonctionnelle coût à minimiser $\mathcal{J}(\phi, c)$, associée à la recherche d'une réduction de traînée ou de bruit, par exemple.
- des contraintes $F(\phi, c) = 0$, qui sont les équations d'état avec les conditions aux limites ou initiales éventuellement.

Pour minimiser la fonctionnelle coût, on introduit une fonctionnelle Lagrangienne qui, à la fonctionnelle coût, ajoute les contraintes multipliées scalairement par des multiplicateurs de Lagrange ξ , qui sont en réalité des variables d'un problème adjoint restant à définir. La minimisation de la fonctionnelle Lagrangienne se fait en calculant les dérivées de Fréchet par rapport à une variation de l'état ϕ , qu'on annule par la suite. Une fois les gradients de la fonctionnelle calculés, on utilise une méthode itérative pour aboutir au contrôle optimal, solution de notre problème. Le calcul des gradients peut aussi être effectué en appliquant la méthode des sensibilités. Il s'agit alors de dériver les contraintes par rapport à la variable de contrôle pour aboutir à la résolution directe d'un système où les dérivées sont les variables principales. Finalement, une discussion sur les intérêts et les inconvénients entre les deux approches conclut cette section :

- différentiation puis discrétisation : en différentiant le système et ses contraintes, on obtient les gradients continus. Ensuite on discrétise l'ensemble du problème pour obtenir la solution numérique.
- discrétisation puis différentiation : on discrétise l'ensemble du problème (contrainte, fonctionnelle), puis on cherche les gradients des grandeurs discrètes par différentiation des équations discrètes.

Contrôle en boucle fermée

Dans cette partie est développée l'approche classique du contrôle optimal avec loi de retour. A partir de mesure des sorties du système, on estime l'état du système optimalement. C'est l'observation et l'estimation. Ensuite, on suppose que l'état estimé est l'état réel, et on bâtit la loi de contrôle, c'est l'étape de contrôle.

Contrôle linéaire quadratique régulier (LQR)

On considère dans un premier temps un système dans le cadre d'information complète, c'est-à-dire, qu'on peut connaître à tout instant l'état du système. Par l'approche adjointe on obtient facilement une loi de contrôle de retour (rétroaction) fonction linéairement de l'état, en minimisant une fonctionnelle basée sur l'état et le coût du contrôle. La solution est en fait obtenue en résolvant une équation de Riccati stationnaire, ce qui signifie qu'on cherche à stabiliser le système sur un horizon infini ($t \rightarrow \infty$).

Dans une seconde étape, sur la base des mesures en sortie, on cherche à reconstruire l'état. Pour cela on applique la théorie du filtre de Kalman-Bucy qui suppose que statistiquement le système est soumis à des bruits gaussiens qui engendrent une erreur dans les mesures. Cette erreur se traduit

par un terme source dit de retour analogue à un contrôle dans l'équation d'estimation de l'état. La minimisation de cette erreur de mesure revient à résoudre une nouvelle équation de Riccati qui permet de trouver la forme du contrôle dans l'équation d'estimation de l'état. On montre en écrivant le système complet (état réel et état estimé) que le problème de contrôle et d'estimation sont duaux.

Contrôle linéaire quadratique gaussien (LQG), \mathcal{H}_2

Cette fois-ci, on considère que l'état réel du système est perturbé par des bruits gaussiens, sur les mesures et sur le contrôle. L'approche et la solution sont identiques au cas précédent. La différence majeure est dans l'introduction du bruit directement dans les équations. Une étude du système complet montre que cela empêche l'état du système de tendre vers une solution complètement stationnaire au bout d'un horizon infini, le bruit gaussien présent alimentant toujours le système.

Contrôle robuste (\mathcal{H}_∞)

Le contrôle robuste est une extension du contrôle LQG. Dans cette approche, la forme du bruit est devenue aussi une inconnue du problème. Le problème d'optimisation devient un problème min max : on cherche le contrôle optimal qui va minimiser la fonctionnelle coût et le pire des bruits qui va maximiser cette même fonctionnelle. La solution est encore basée sur deux équations de Riccati, mais des matrices supplémentaires relatives à l'influence du bruit dans le contrôle et les mesures interviennent. Une brève présentation de l'utilisation du contrôle en boucle fermée conclut cette section.

2.1 Introduction

This chapter summarizes the various tools from control theory. The results from this chapter are used in this thesis, while performing the LQG control on our ROM. Also the method of adjoint as introduced in this chapter is evoked on numerous occasions, in chapters on calibration, sensitivity analysis of the ROM, linearization of the model while performing feedback. To introduce the basic ideas we closely follow the work contained in [Zabczyk \(1996\)](#), and [Evans \(1983\)](#). For the application of the control theory in fluid mechanics an exhaustive treatment can be found in [Bewley & Agarwal \(1996\)](#), [Bewley & Liu \(1998\)](#), [Kim & Bewley \(2007\)](#) and more recently [Bagheri et al. \(2009b\)](#). To begin with we introduce the various terms frequently encountered in the control theory. The starting point of control theory is the differential equation

$$\dot{x}(t) = f(x, u), \quad x(0) = x_0 \in \mathbb{R}^n \quad (2.1)$$

with the right-hand side depending on a parameter u from a set $\mathcal{U} \subset \mathbb{R}^m$ called as the set of control parameters. An important question in the theory of differential equations is the continuous dependence of solutions on parameters and has been answered under appropriate conditions. In control theory we pose questions of different type, and depending on the nature of the control two definitions of control can be found: *open loop* and *closed loop*. An *open loop* control is basically an arbitrary function $u(\cdot) : [0, +\infty) \rightarrow \mathcal{U}$ for which the equation

$$\dot{x}(t) = f(x(t), u(t)), \quad t \geq 0, x(0) = x_0 \quad (2.2)$$

has a well defined solution. A *closed loop* control is a mapping $k : \mathbb{R}^n \rightarrow \mathcal{U}$ which may depend of time $t \geq 0$, such that the equation

$$\dot{x}(t) = f(x(t), k(x(t))), \quad t \geq 0, x(0) = x_0 \quad (2.3)$$

has a well defined solution. The mapping $k(\cdot)$ is called *feedback*. Control are also called the *inputs* of the system and the corresponding solutions of (2.2) or (2.3) are called the *outputs* of the system.

Controllability

A state $z \in \mathbb{R}^n$ is said to be *reachable* from x in time T , if there exists an open loop control $u(\cdot)$ such that, for the output $x(\cdot)$, $x(0) = x_0, x(T) = z$. If the state z is reachable from an arbitrary state x in time T , then the system (2.1) is controllable. In many cases we require transferring an arbitrary state into the given one, in particular the origin. The effective characterisation of controllable systems is a partially solved problem in control theory.

Stabilizability

An important issue is that of stabilizability. If for some $\bar{x} \in \mathbb{R}^n$ and $\bar{u} \in \mathcal{U}$, $f(\bar{x}, \bar{u}) = 0$. A function $k : \mathbb{R}^n \rightarrow \mathcal{U}$ such that $k(\bar{x}) = \bar{u}$ is called a *stabilizing feedback* if \bar{x} is a stable equilibrium for the

system.

$$\dot{x}(t) = f(x(t), k(x(t))), \quad t \geq 0, x(0) = x_0$$

There exist many methods to determine whether a given equilibrium state is a stable one.

Observability

In many practical situations one observes not the state $x(t)$ but its function $h(x(t)), t \geq 0$. It is therefore necessary to consider the pair of equations

$$\dot{x} = f(x, u), \quad x(0) = x_0 \quad (2.4)$$

$$y = h(x) \quad (2.5)$$

equation (2.5) is called an observation equation. The system is (2.4)-(2.5) is said to be *observable* if, knowing a control $u(\cdot)$ and an observation $y(\cdot)$, on a given interval $[0, T]$, one can determine uniquely the initial condition x .

Optimality

In control theory besides the above questions of structural character one also asks optimality questions. In the time optimal problem we seek a control which transfers a state x onto z in a minimal time T . In other problems the time T is fixed and one seeks a control $u(\cdot)$ which minimises the integral

$$\mathcal{J}(x, u) = \int_0^T P(x(t), u(t)) dt + Q(x(t))$$

where P and Q are given functions. The methods of control theory can be broadly classified based on the right hand side of the system (2.4) being linear or non-linear where we describe the control as linear or non-linear. In case of non-linear control problems subjected to constraints the method of Lagrange multipliers is well known as described in [Gunzburger \(1997a\)](#), [Gunzburger \(1997b\)](#), [Gunzburger \(1997c\)](#). The method is described in the next section and is largely inspired from [Gunzburger \(1997a\)](#).

2.2 Open loop control and constrained optimisation

Most of the flow control or optimisation problem can be set in an abstract setting for which we define the following

1. *state variables* ϕ : which are described by the governing equations, such as velocity, pressure, temperatures etc.

2. Basic tools from control theory

2. The *control* c which is usually introduced as an external source, such as mass influx, heating on the boundary.
3. *cost functional*: $\mathcal{J}(\phi, c)$ which is the desired objective we want to achieve by the application of control such as minimisation of the exit energy, reduction in noise, drag, etc.
4. The *constraint* $F(\phi, c) = 0$ is the flow equations or any side constraint to be satisfied such as the initial or boundary condition.

The constrained optimisation problem is then to find controls c and states ϕ such that $\mathcal{J}(\phi, c)$ is minimised (or maximised), subject to the constraint $F(\phi, c) = 0$. In many cases the functional to be minimised do not explicitly depend on the control parameters, resulting in ill-posed problems [Gunzburger \(1997c\)](#). This may force one to restrict the size of the control, which can be done two-fold

1. Limit the size of the control so that one looks for optimal control within a bounded set, e.g., one could look for optimal controls such that under some suitable norm

$$\|c\| \leq M$$

2. To penalize the objective functional with some norm of the control so that the new functional becomes

$$\mathcal{J}(\phi, c) = \varepsilon(\phi) + \ell^2 \|c\|^2 \quad (2.6)$$

The parameter ℓ is chosen empirically. The smaller the value of ℓ the more the control available to make the first term small which is presumably the goal of the optimisation. This strategy is easier to implement than the earlier one which results in variational inequalities.

In the method of Lagrange multipliers to enforce constraints we introduce an adjoint or co-state variable ξ to define a new objective functional

$$\mathcal{L}(\phi, c, \xi) = \mathcal{J}(\phi, c) - \langle F(\phi, c), \xi \rangle \quad (2.7)$$

where $\langle \cdot \rangle$ denotes an appropriate inner product which depends on the setting of the problem. The constrained optimisation problem can be stated as finding

To find controls c , states ϕ and co-states ξ such that $\mathcal{L}(\phi, c, \xi)$ is stationary. The above definition of the functional (2.7) ensures that each argument is independent of the other contrary to the original problem in which the argument had to satisfy $F(\phi, c) = 0$. The Lagrangian functional \mathcal{L} admits an extremum at the stationary points of \mathcal{L} which is obtained by setting the first variation of \mathcal{L} with respect to each variable $\delta\mathcal{L} = 0$ i.e.

$$\delta\mathcal{L} = \frac{\partial\mathcal{L}}{\partial\phi}\delta\phi + \frac{\partial\mathcal{L}}{\partial c}\delta c + \frac{\partial\mathcal{L}}{\partial\xi}\delta\xi = 0 \quad (2.8)$$

We suppose that the variables ϕ , c , ξ are independent ¹ and the Fréchet derivative ² with respect to each variable is identically equal to 0 with respect to each variables ϕ , c , and ξ . *i.e.*

$$\frac{\partial \mathcal{L}}{\partial \phi} \delta \phi = \frac{\partial \mathcal{L}}{\partial c} \delta c = \frac{\partial \mathcal{L}}{\partial \xi} \delta \xi = 0$$

The expressions above represents a necessary and sufficient conditions for the determination of an extremum in case the functional is convex and gives a local extremum of the functional. We do not consider the global optimisation methods as they are too expensive in fluid dynamic computation, and is still an active area of research as found in the works of [Mohammadi \(2007\)](#), [Mohammadi & Pironneau \(2004\)](#). The local optimisation methods may be stuck in a local extremum, which may not be of interest. Also the presence of many local extrema may seriously affect the performance of the algorithm. Global optimisation method such as genetic algorithms is still less utilised in the field of fluid dynamic optimisation as the number of parameters is limited applications, as can be found in [Quagliarella & Vicini \(1997\)](#), [Obayashi \(1997\)](#), [Makinen *et al.* \(1999\)](#). Setting the first variation of \mathcal{L} with respect to the Lagrange multiplier ξ equal to zero gives

$$\begin{aligned} \frac{\partial \mathcal{L}}{\partial \xi} \delta \xi &= \lim_{\epsilon \rightarrow 0} \frac{\mathcal{L}(\phi, c, \xi + \epsilon \delta \xi) - \mathcal{L}(\phi, c, \xi)}{\epsilon} = 0 \\ &= \lim_{\epsilon \rightarrow 0} \frac{-\langle F(\phi, c), \xi + \epsilon \delta \xi \rangle + \langle F(\phi, c), \xi \rangle}{\epsilon} = 0 \end{aligned}$$

Where the variation $\delta \xi$ is arbitrary. On simplification we obtain

$$\langle F(\phi, c), \delta \xi \rangle = 0$$

or

$$F(\phi, c) = 0 \tag{2.9}$$

which is nothing but the equation of state, which is the constraint of the optimisation problem. Setting the first variation of \mathcal{L} with respect to the state ϕ in the direction $\delta \phi$ yields

$$\begin{aligned} \frac{\partial \mathcal{L}}{\partial \phi} \delta \phi &= \lim_{\epsilon \rightarrow 0} \frac{\mathcal{L}(\phi + \epsilon \delta \phi, c, \xi) - \mathcal{L}(\phi, c, \xi)}{\epsilon} = 0 \\ &= \lim_{\epsilon \rightarrow 0} \left[\frac{\mathcal{J}(\phi + \epsilon \delta \phi, c) - \mathcal{J}(\phi, c)}{\epsilon} - \frac{\langle F(\phi + \epsilon \delta \phi, c), \xi \rangle - \langle F(\phi, c), \xi \rangle}{\epsilon} \right] = 0 \end{aligned}$$

¹Rigorously speaking this is not a fully correct assumption as the control and the state variables, c , ϕ are related by the equation of state $F(\phi, c) = 0$.

²The Fréchet derivative of \mathcal{L} at the point x_0 in the direction δx is given by

$$\lim_{\epsilon \rightarrow 0} \frac{\mathcal{L}(x_0 + \epsilon \delta x) - \mathcal{L}(x_0)}{\epsilon}$$

2. Basic tools from control theory

We consider the Taylor series expansion upto order $O(\epsilon)$, the above relation becomes

$$\lim_{\epsilon \rightarrow 0} \left(\frac{\partial \mathcal{J}}{\partial \phi} \delta \phi - \left\langle \frac{\partial F}{\partial \phi} \delta \phi, \xi \right\rangle + O(\epsilon) \right)$$

On further simplification

$$\frac{\partial \mathcal{J}}{\partial \phi} \delta \phi - \left\langle \frac{\partial F}{\partial \phi} \delta \phi, \xi \right\rangle = 0$$

The first term can be written in terms of the inner product as

$$\left\langle \frac{\partial \mathcal{J}}{\partial \phi} \delta \phi, 1 \right\rangle - \left\langle \frac{\partial F}{\partial \phi} \delta \phi, \xi \right\rangle = 0$$

On using the definition of the adjoint denoted by $(\cdot)^*$:

$$\left\langle \delta \phi, \left(\frac{\partial \mathcal{J}}{\partial \phi} \right)^* \right\rangle - \left\langle \delta \phi, \left(\frac{\partial F}{\partial \phi} \right)^* \xi \right\rangle = 0$$

Since the variation $\delta \phi$ is arbitrary we obtain the adjoint or co-state equations

$$\left(\frac{\partial F}{\partial \phi} \right)^* \xi = \left(\frac{\partial \mathcal{J}}{\partial \phi} \right)^* \quad (2.10)$$

Note that the adjoint equations are linear in the adjoint variables ξ . In fact the adjoint of the state equations are linearised about the state. Finally setting the variation of the \mathcal{L} with respect to the control c in the direction δc yields

$$\begin{aligned} \frac{\partial \mathcal{L}}{\partial c} \delta c &= \lim_{\epsilon \rightarrow 0} \frac{\mathcal{L}(\phi, c + \epsilon \delta c, \xi) - \mathcal{L}(\phi, c, \xi)}{\epsilon} = 0 \\ &= \lim_{\epsilon \rightarrow 0} \left[\frac{\mathcal{J}(\phi, c + \epsilon \delta c) - \mathcal{J}(\phi, c)}{\epsilon} - \frac{\langle F(\phi, c + \epsilon \delta c), \xi \rangle - \langle F(\phi, c), \xi \rangle}{\epsilon} \right] = 0 \end{aligned}$$

As previously, we consider the Taylor series expansion upto order $O(\epsilon)$ to obtain

$$\frac{\partial \mathcal{J}}{\partial c} \delta c - \left\langle \frac{\partial F}{\partial c} \delta c, \xi \right\rangle = 0$$

On introducing the inner product for the first term

$$\left\langle \frac{\partial \mathcal{J}}{\partial c} \delta c, 1 \right\rangle - \left\langle \frac{\partial F}{\partial c} \delta c, \xi \right\rangle = 0$$

again introducing the adjoint operator we have

$$\left\langle \delta c, \left(\frac{\partial \mathcal{J}}{\partial c} \right)^* \right\rangle - \left\langle \delta c, \left(\frac{\partial F}{\partial c} \right)^* \xi \right\rangle = 0$$

Finally the optimality condition is given as

$$\left(\frac{\partial F}{\partial c}\right)^* \xi = \left(\frac{\partial \mathcal{J}}{\partial c}\right)^* = \ell^2 c \quad (2.11)$$

System (2.9)-(2.11), also called as the Euler-Lagrange equations are a system of coupled partial differential equations whose solution yields the optimal control c , the optimal state ϕ and the optimal co-state ξ . The coupled system is more complicated than the original system and computationally expensive to obtain the solution directly (also called "The one shot method"), especially in the case of computational fluid dynamics where the number of degrees of freedom can go upto the order of 10^7 . One therefore resorts to an iterative method in which one iterates between different equations, the algorithm for which can be summarized as below.

1. for $n = 0$ initialise the guess value for the control $c^{(0)}$.
2. Solve $F(\phi^{(n)}, c^{(n)})$ (2.4) to obtain the state $\phi^{(n)}$
3. Determine the adjoint state $\xi^{(n)}$ by resolving equation (2.10) as

$$\left(\frac{\partial F}{\partial \phi}\right)^{*(n)} \xi^{(n)} = \left(\frac{\partial \mathcal{J}}{\partial \phi}\right)^{*(n)}$$

4. The new control $c^{(n+1)}$ is obtained by solving the optimality condition (2.11) to obtain the gradient

$$\left(\frac{\partial \mathcal{J}}{\partial c}\right)^{*(n)} = \left(\frac{\partial F}{\partial c}\right)^{*(n)} \xi$$

5. The new value of the control is obtained as

$$c^{(n+1)} = c^{(n)} + s^{(n)} \left(\frac{\partial \mathcal{J}}{\partial c}\right)^{*(n)}$$

where $s^{(n)}$ is the step length of descent obtained from any descent algorithm.

6. iterate the above step till a convergence criteria is satisfied

We remark that the above iterative algorithm is equivalent to the method of steepest descent for the unconstrained functional $\mathcal{J}(\phi(c), c)$ where $\phi(c)$ is the state corresponding to the control c . One important component of the optimisation problem is the determination of the gradient in step 4, which can be obtained by different methods as will be explained in the next section. Since the main aspect is the calculation of the state variables, we wish to keep the number of computation small and the principle of model reduction is one such strategy.

2.2.1 Functional gradients through sensitivities

To determine the functional gradient in step 3 of the algorithm, we use the chain rule to obtain

$$\frac{d\mathcal{J}(\phi, c)}{dc} = \frac{\partial\mathcal{J}(\phi, c)}{\partial\phi} \frac{d\phi}{dc} + \frac{\partial\mathcal{J}(\phi, c)}{\partial c} \quad (2.12)$$

Since the functional \mathcal{J} depends explicitly on ϕ and c , the terms $\frac{\partial\mathcal{J}}{\partial\phi}$ and $\frac{\partial\mathcal{J}}{\partial c}$ can be determined easily. Since the state variable ϕ depends implicitly on the control parameter c it is more subtle to determine the sensibility $\frac{d\phi}{dc}$. A simple idea is to use a finite difference approximation given by

$$\left. \frac{d\phi}{dc} \right|_{c^n} \approx \frac{\phi(c^n) - \phi(\tilde{c})}{c^n - \tilde{c}} \quad (2.13)$$

where \tilde{c} is a value in the neighborhood of c^n and $\phi(\tilde{c})$ is a solution of the state equation at \tilde{c} *i.e.* $F(\phi(\tilde{c}), \tilde{c}) = 0$. This is a costly solution as it is required to solve an additional nonlinear state equation for each sensitivities and is prone to inaccuracies. A better method to determine the sensitivities is to differentiate the constraint equation $F(\phi, c) = 0$ again by chain rule to obtain a linear system for sensitivities as

$$dF = \frac{\partial F}{\partial\phi} d\phi + \frac{\partial F}{\partial c} dc = 0 \quad (2.14)$$

therefore

$$\left(\frac{\partial F}{\partial\phi} \right) \left. \frac{d\phi}{dc} \right|_{c^n} = - \left. \frac{\partial F}{\partial c} \right|_{c^n} \quad (2.15)$$

The major disadvantage of this method is to resolve a linear system with the optimal parameters. The terms $\left. \frac{\partial F}{\partial\phi} \right|_{c^n}$ and $\left. \frac{\partial F}{\partial c} \right|_{c^n}$ can be determined at the beginning of the iteration just after the resolution of the state.

2.2.2 Functional gradients using adjoint equations

One can also use the adjoint equations to determine the gradients of the functional. To demonstrate we write the adjoint equation (2.10) for the sake of convenience as

$$\left(\frac{\partial F}{\partial\phi} \right)^* \xi = \left(\frac{\partial\mathcal{J}}{\partial\phi} \right)^*$$

which is equivalent to the equation

$$\xi^* \frac{\partial F}{\partial\phi} = \frac{\partial\mathcal{J}}{\partial\phi} \quad (2.16)$$

Substituting this in equation (2.12) we obtain

$$\frac{d\mathcal{J}(\phi, c)}{dc} = \xi^* \frac{\partial F(\phi, c)}{\partial c} \frac{d\phi}{dc} + \frac{\partial\mathcal{J}(\phi, c)}{\partial c} \quad (2.17)$$

Finally on using 2.15

$$\frac{d\mathcal{J}(\phi^n, c^n)}{dc} = -(\xi^n)^* \frac{\partial F}{\partial c}|_{c^n} + \frac{\partial \mathcal{J}}{\partial c}|_{c^n} \quad (2.18)$$

The advantage of this method is that to determine the sensitivities, we need to resolve the adjoint system once independent of the number of optimal parameters. Also the adjoint of the optimality condition (2.11) is valid for non zero values of the gradient of the cost functional $\frac{d\mathcal{J}}{dc}$. When the optimality condition is satisfied we have $\frac{d\mathcal{J}}{dc} = 0$. For problems with many design parameters this approach is much cheaper than using sensitivities. However sensitivities are useful in their own right as they help in determining how a variation in a parameter affect the flow.

2.2.3 Differentiation then Discretisation

Sensitivities can be determined in two ways. One can differentiate the continuous flow system at the partial differential equation (PDE) level to obtain a system of equations for sensitivities and then discretise the continuous sensitivity system. Alternatively one can also discretise the continuous flow equations and then differentiate to obtain the sensitivities of the discrete system. It is also worthwhile to note that the differentiation and discretisation process do not commute and yields a different approximation to the sensitivities. The difference between the two approach can be summarized in figure 2.1. In the following section we give a brief discussion between the two approaches.

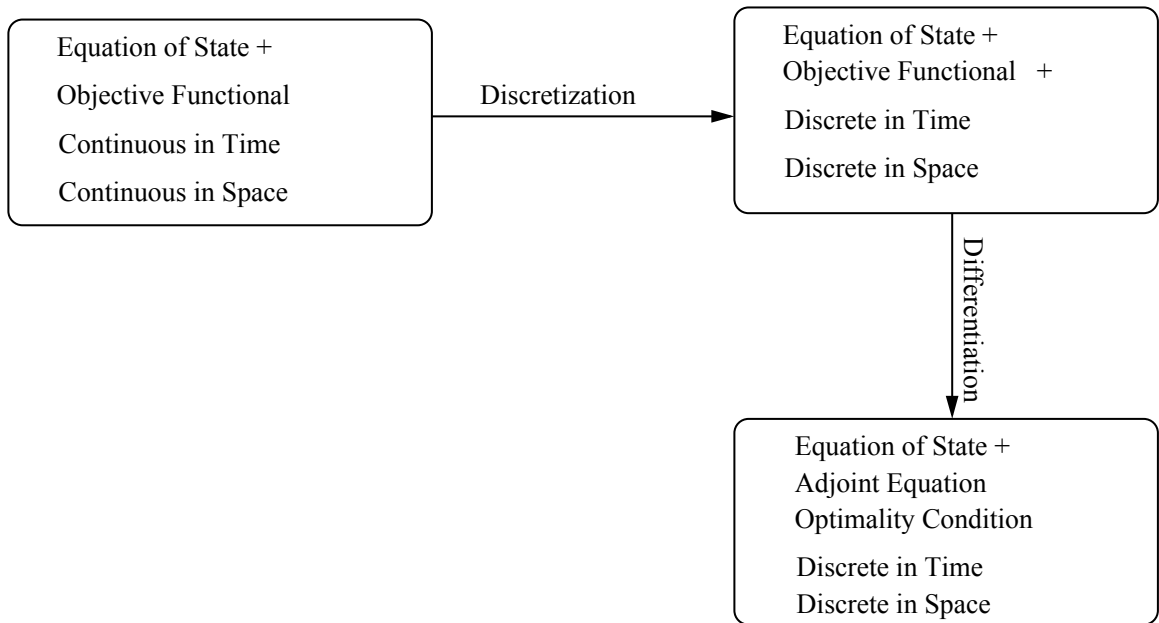
2.2.4 Discretisation-Differentiation

This approach consists of discretizing the equation of state and then differentiating the discrete expression to obtain the gradients. The main advantage of this method is the sensitivities of the optimisation problem are obtained exactly. Contrary to the case of discretisation-differentiation approach there is no need of calculating new solutions of the discretised equations. This method requires a choice of parameter in the code and returns a new code which computes the approximate parameters and exact sensitivities without any user intervention. Although this method has gained some popularity in field like shape optimisation it has been very less utilised for fluid dynamic problems [Hinze & Slawing \(2003\)](#) is one such work. The overhead cost of this operation is very large as it requires more CPU time than the differentiate-discretisation approach.

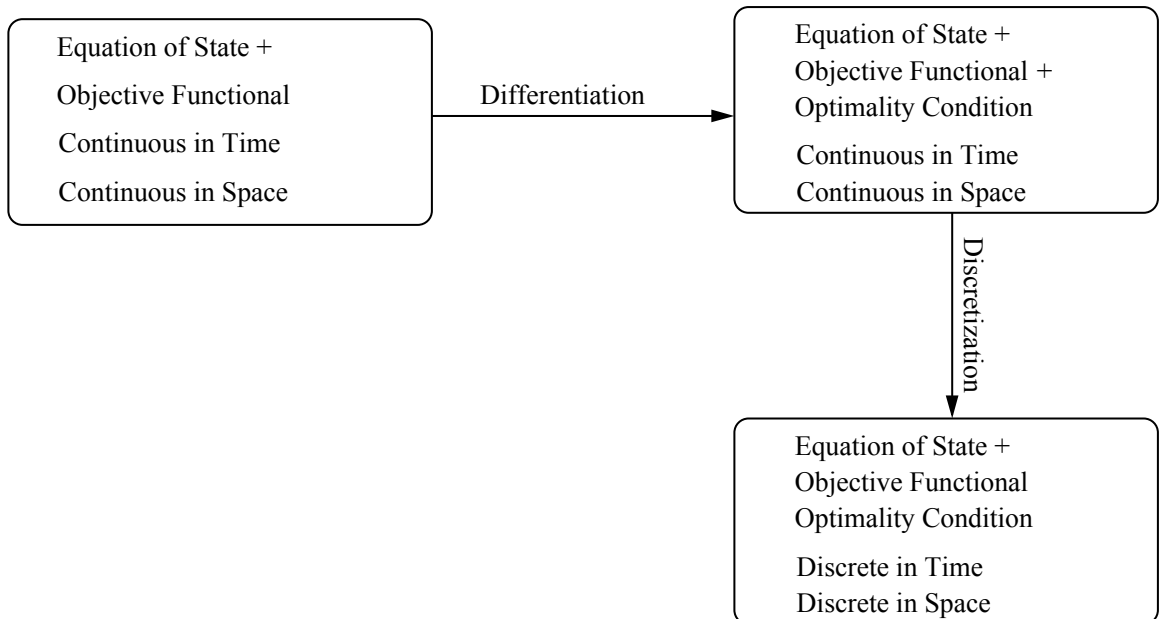
2.2.5 Differentiation-Discretisation

In this approach the continuous state system is differentiated with respect to the parameters to yield a continuous system of equations for sensitivities of the exact solution with respect to the parameter. The sensitivities then might be discretized with respect to the given parameter to obtain an approximation for the exact sensitivities. Although the approach is cost effective, the difficulty lies in approximating the sensitivities as they are not the exact derivatives of anything. This leads to inconsistent gradients of functional *i.e.* the approximate gradient is not the true gradient of anything. Also in applications where inherent discontinuities in the solution are present such as shocks the approach

2. Basic tools from control theory



(a) Differentiation then discretisation



(b) Discretisation then differentiation

Figure 2.1 - Schematic representation of the different approaches of resolution of the optimal system. Discussion of the commutativity between the discretisation and differentiation operator.

need not be feasible as the weak solution of the shock namely the Rankine-Hugoniot condition need to be considered as a constraint [Castro et al. \(2008\)](#), [Bardos & Pironneau \(2003\)](#). In literature we do

find a large application of this method in the fluid dynamic context notably in [Bewley & Liu \(1998\)](#), [Walther *et al.* \(2001\)](#), [Spagnoli & Airiau \(2008\)](#), [Shrif. \(2008\)](#), [Marquet *et al.* \(2008\)](#) and will be used for the later developments in the context of reduced order modelling. An interesting study of comparison of the various adjoint techniques is found in [Noack & Walther \(2007\)](#) where the difference between the discrete adjoint and continuous adjoint are compared.

2.3 Feedback control

In this section we demonstrate the principles of a feedback control. The control on the physical system can be applied by computing the effect of control in advance such that the desired state of the physical system is achieved. This strategy is known as open-loop control. However when there are disturbances in the physical system, due to the presence of uncertainties open-loop control fails to give the desired effect. Closed-loop control or feedback control is based on the concept that one is able to monitor the model by means of output measurements and establishes a connection between the measurements and the input of the system. Figure 2.2 illustrates the concept of a feedback control. Here P is the plant that describes our model and is usually given by a dynamical system of the form

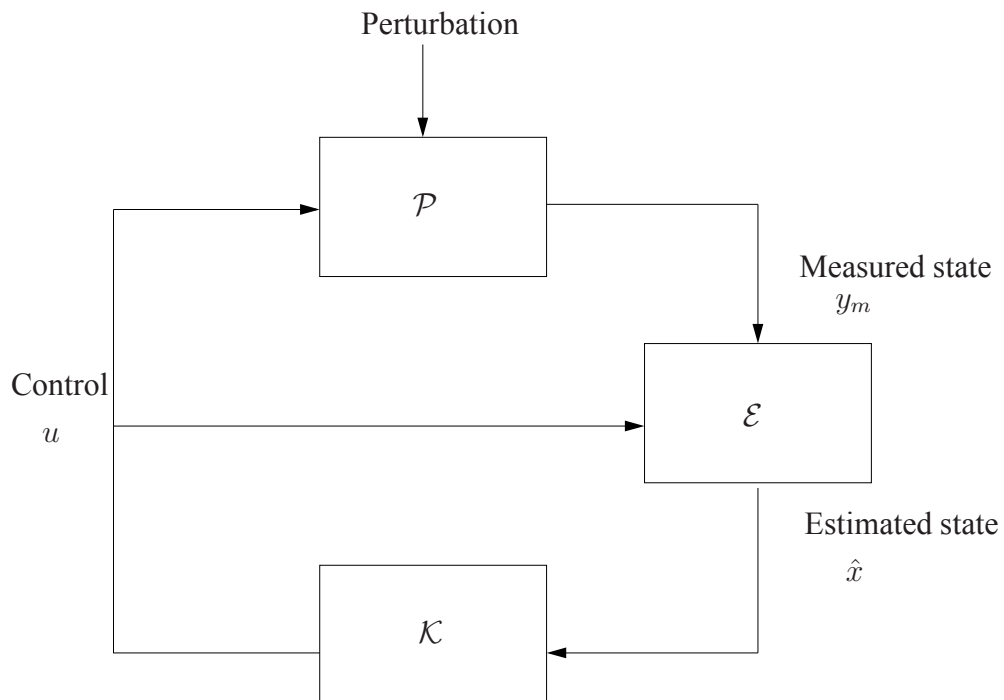


Figure 2.2 - Block diagram of control with estimation

$$\dot{x} = Ax + Bu \quad (2.19a)$$

$$y_m = Cx + Du \quad (2.19b)$$

Where the matrix A also known as the state matrix determines the evolution of the state x , the control u is applied to the system to drive the state towards zero, the control is based on measurements y_m . The matrices B, C, D are mainly problem dependent and depends on the way the control is applied (weather a boundary control or an internal forcing) and the way the measurements are made. In many cases the state is an internal variable and cannot be observed. Instead a few noisy measurements \hat{y}_m are made, and used to estimate the state \hat{x} , which is then fed to the controller to determine the control u which is then applied back to the plant to drive the state towards zero. The estimation problem can be stated more precisely as follows

$$\dot{\hat{x}} = A\hat{x} + Bu - \hat{u} \quad (2.20a)$$

$$\hat{y}_m = C\hat{x} + Du \quad (2.20b)$$

$$\hat{u} = \mathcal{L}(y_m - \hat{y}_m) \quad (2.20c)$$

Where \hat{u} can be interpreted as forcing applied to the plant \mathcal{P} and \hat{y}_m denotes the measurement associated with the state \hat{x} . Once the state \hat{x} has been determined using the estimator \mathcal{E} the control can be determined as

$$u = -\mathcal{K}(\hat{x}) \quad (2.21)$$

The problem now lies in determining the operators \mathcal{L}, \mathcal{K} such that the term \hat{u} forces the state variable \hat{x} toward the actual state x and the control u drives the state x towards zero. The equivalent criteria for determining the controllability and Observability for a finite dimensional system is discussed in appendix A. We present the methods in section §2.4, and section §2.5 the different strategies of determining the control, based on the solution of the Ricatti equation. Based on the functional space in which the optimisation problem is solved the control can be classified as \mathcal{H}_2 and \mathcal{H}_∞ which will be discussed in the next section. For details one can refer [Lewis & Syrmos \(1995\)](#), [Bewley & Agarwal \(1996\)](#), [Zhou et al. \(1996\)](#), [Kim & Bewley \(2007\)](#).

2.4 \mathcal{H}_2 control theory

2.4.1 Linear Quadratic Regulator LQR control

One considers a linear system continuous, invariant in time of the form.

$$\dot{x} = Ax + Bu \quad (2.22a)$$

$$u = -K_{LQR}x \quad (2.22b)$$

with x representing the state, u representing the control law, the second equation represents the feedback law. We assume that there is no external disturbances and we are able to measure the full state. The LQR consists is to find a control law that stabilises the system (2.22), and minimises the cost functional given by

$$\mathcal{J}_{LQR} = \frac{1}{2} \int_0^\infty (x^T Q x + u^T R u) dt \quad (2.23)$$

where the weight matrices Q, R are assumed positive definite. The control is found out in knowing the full information in that the state of the system at the input and output is known in advance for all time. As in the previous section we introduce the Lagrange multipliers ξ to define the augmented functional

$$\mathcal{L} = \int_0^\infty \left(\frac{1}{2} x^T Q x + \frac{1}{2} u^T R u - \xi^T [\dot{x} - Ax - Bu] \right) dt \quad (2.24)$$

Variation of the above functional gives

$$\delta \mathcal{L} = [-\xi^T \delta x]_0^\infty + \int_0^\infty (\{x^T Q + \xi^T A + \dot{\xi}^T\} \delta x + \{u^T R + \xi^T B\} \delta u) dt \quad (2.25)$$

The minimisation is achieved if

$$\dot{\xi} = -A^T \xi - Qx \quad (2.26)$$

$$u = -R^{-1} B^T \xi \quad (2.27)$$

$$[-\xi^T \delta x]_0^\infty = 0 \quad (2.28)$$

We assume a linear relation between the state and the adjoint variable as

$$\xi = X(t)x \quad (2.29)$$

where X is any positive definite matrix. The feedback law (2.27) becomes

$$K_{LQR} = R^{-1} B^T X \quad (2.30)$$

On using (2.22) and (2.29), equation (2.26) becomes

$$X\dot{x} + \dot{X}x = -(A^T X + Q)x = \dot{X}x + X(Ax + Bu) = \dot{X}x + X(Ax + B[-R^{-1} B^T Xx])$$

This equation is verified for some value of x , if X is the solution of Riccati equation given

$$-\dot{X} = A^T X + XA + Q - XBR^{-1}B^T X \quad (2.31)$$

In general the infinite time horizon problem is solved by taking the term $\dot{X} = 0$ in (2.31)

2.4.2 Lyapunov equation and minimum of the functional \mathcal{J}_{LQR}

The functional \mathcal{J}_{LQR} being a scalar can be written using the feedback law as

$$\begin{aligned} \mathcal{J}_{LQR} &= \text{Trace} \left[\int_0^\infty \left(\frac{1}{2} x^T Q x + \frac{1}{2} u^T R u \right) dt \right] = \frac{\text{Trace}}{2} \left[\int_0^\infty (x^T (Q + K_{LQR}^T R K_{LQR}) x) dt \right] \\ &= \frac{\text{Trace}}{2} [(Q + K_{LQR}^T R K_{LQR}) L] \end{aligned} \quad (2.32)$$

2. Basic tools from control theory

Where the matrix $L = \int_0^\infty x x^T dt$. The equation of state can be now written as

$$\dot{x} = A_f x \quad \text{with} \quad A_f = A - BK_{LQR}$$

The solution of the above equation can be characterised as

$$x(t) = \exp(A_f t) x_0$$

We now recall a result from the Lyapunov theory which states that the above system is asymptotically stable if

$$A_f L + L A_f^T = -x_0 x_0^T$$

It can be shown that using the equation of state and the Riccati equation $X A_f + A_f^T X = -(Q + K_{LQR}^T R K_{LQR})$, the minimum of the functional is given as

$$\mathcal{J}_{min} = \frac{\text{Trace}}{2} [(Q + K_{LQR}^T R K_{LQR})L] = -\frac{\text{Trace}}{2} [(X A_f + A_f^T X)]$$

where $\mathcal{J} = \mathcal{J}_{LQR}$ for notational convenience. On observing that $\text{Trace}(AB) = \text{Trace}(BA)$ and $\text{Trace}(A + B) = \text{Trace}(A) + \text{Trace}(B)$ the minimum can be written as

$$\mathcal{J}_{min} = \frac{1}{2} x_0^T X x_0 \tag{2.33}$$

A typical LQR plant model can be summarized as shown in the figure 2.3

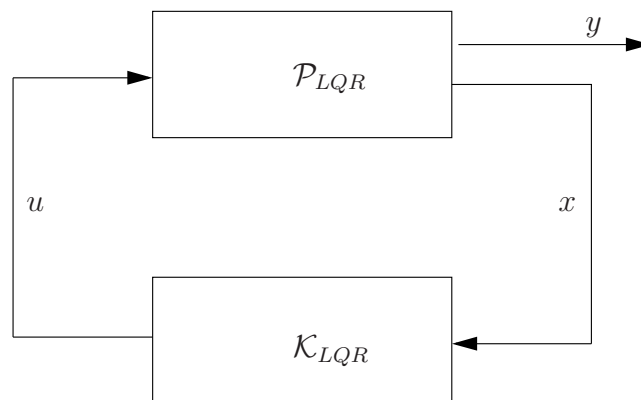


Figure 2.3 - Typical block diagram of an LQR control

2.4.3 Estimation and the Kalman-Bucy Filter (KBF)

In real time systems it is often natural to encounter external disturbances that enter into the system and hence the state is not precisely known. For example when acoustic measurements of flow are

made using a microphone one can expect the presence of the instrument noise affecting the measurement. This leads us to the estimation problem in which the state (a part of it) needs to be estimated before designing the control. The Kalman-Bucy Filter (KBF) is a well known tool for the estimation problem. The external disturbances for the state w_1 and the measurements w_2 is assumed to be uncorrelated white Gaussian process with zero mean and the covariance matrix defined by $E[w_1^*w_1] = I$, $E[w_2^*w_2] = I$, where $E[\cdot]$ is any expectation operator. We define the square root of the covariance of the disturbance to the state equation and measurements by G_1, G_2 respectively. The system \mathcal{P} can be written as

$$\dot{x} = Ax + G_1w_1 + B_2u \quad (2.34a)$$

$$y_m = Cx + G_2w_2 + Du \quad (2.34b)$$

The objective of the Kalman Bucy Filter is to estimate the state x as accurately as possible based on the measurements y_m . In other words the KBF tries to minimise the estimation error e_x defined by

$$e_x = x - \hat{x} \quad (2.35)$$

where the state \hat{x} is determined using a filter. The cost functional can be written as

$$\mathcal{J}_{KBF} = E[\|\chi_e\|^2]$$

where $\chi_e \equiv e_x$ for the sake of notation, and E is any expectation operator³. For the sake of generalisation in latter sections we introduce the following notations, assuming G_2 nonsingular. The disturbance vector can be defined as

$$w = \begin{pmatrix} w_1 \\ w_2 \end{pmatrix}$$

we also define

$$B_1 \equiv (G_1, 0) \quad C_2 \equiv G_2^{-1}C \quad D_{21} \equiv (0, I)$$

On using a simple change of variable the observation vectors y, \hat{y} is defined as

$$y \equiv G_2^{-1}(y_m - Du) \quad \hat{y} \equiv G_2^{-1}(\hat{y}_m - Du)$$

With the change of variable (2.34) and (2.20) can be written as

$$y = C_2x + D_{21}w \quad (2.36a)$$

$$\hat{y} = C_2\hat{x} \quad (2.36b)$$

³The definition of the functional by means of an integral on $t \in [0, \infty]$ is not convenient due to the problem of convergence, the expectation being the suitable measure.

2. Basic tools from control theory

It is also appropriate to define the output estimation error $e_y \equiv y - \hat{y}$. The equations for the state estimation error and output estimation error can be written by the definition of errors e_x , e_y and equations (2.20), (2.36) as

$$\dot{e}_x = Ae_x + B_1w + \hat{u} \quad (2.37a)$$

$$\chi_e = e_x \quad (2.37b)$$

$$e_y = C_2e_x + D_{21}w \quad (2.37c)$$

The Kalman-Bucy estimator matrix \mathcal{L}_{KBF} is estimated such that the control \hat{u} , forces the state variable of the estimation error \hat{e}_x towards the minimisation of $\mathcal{J}_{KBF}(\chi_e)$ in the presence of disturbances w . The above facts can be written in a shorthand form as shown in table. Where \mathcal{P}_{KBF} represents the

$$\mathcal{P}_{KBF} = \begin{array}{c} \dot{e}_x \\ \chi_e \\ e_y \end{array} \begin{array}{c} = \\ \\ \\ \end{array} \begin{array}{c} \left| \begin{array}{c|cc} & e_x & w & \hat{u} \\ \hline & A & B_1 & I \\ \hline & I & 0 & 0 \\ \hline & C_2 & D_{21} & 0 \end{array} \right| \end{array}$$

plant and \mathcal{L}_{KBF} represents the filter gain. We introduce the Hamiltonian as

$$H_{KBF} = \begin{pmatrix} A^T & -C^T C \\ -B_1 B_1^T & -A \end{pmatrix}$$

The Ricatti equation associated with H_{KBF} can be written as

$$AY^T + YA^T - Y(C_2^T C_2)Y + (B_1 B_1^T) = 0 \quad (2.38)$$

also denoted by $Y = \text{Ric}(H_{KBF})$. Note that the gain obtained from the KBF is the dual of the gain obtained from the LQR control described in (2.31). The feedback operator L can be written as

$$L = -YC_2^T \quad (2.39)$$

and the Kalman-Bucy filter \mathcal{L}_{KBF} given by

$$\hat{u} = Le_y = -YC_2^T e_y \quad (2.40)$$

The estimator \hat{y} is given by the equation

$$\dot{\hat{y}} = A\hat{x} + B_2u - L(y - C_2\hat{x}) \quad (2.41)$$

and minimises $E(\|e_x\|^2)$ for a system with Gaussian disturbances. The block diagram of the KBF can be summarized as shown in figure 2.4.3

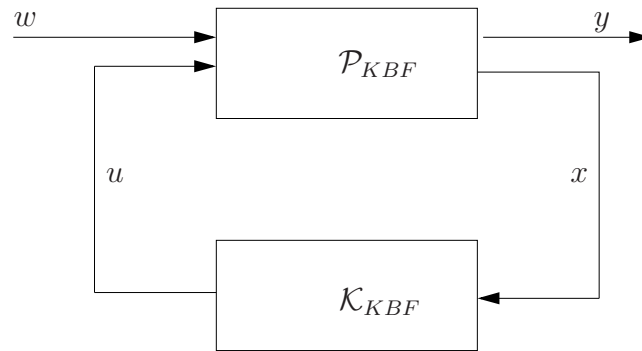


Figure 2.4 - Block diagram of Kalman Filter.

2.4.4 Linear Quadratic Gaussian LQG control

We combine the results obtained from LQR for the control and the KBF for the estimation part to obtain a system \mathcal{P}_{LQG} subjected to Gaussian disturbances. The cost functional for minimisation can be written as

$$\mathcal{J}_{LQG} = E [\|x\|^2 + \ell^2 u^2] \quad (2.42)$$

Note that $Q = I$ and $R = \ell^2$ in the definition of (2.23), $\|\cdot\|$ represents the euclidian norm or the L_2 norm. The functional (2.42) can be written in a form similar to that of the Kalman-Bucy filter by introducing the transformation variable

$$\chi = \begin{pmatrix} Q^{1/2}x/\ell \\ u \end{pmatrix}$$

to obtain the new functional of minimisation as

$$\mathcal{J}_{LQG} = E[\|\chi\|^2] \quad (2.43)$$

The term LQG comes from the fact that the plant being linear, the cost functional being quadratic, and the external disturbances being Gaussian. Using the same way the plant (2.34) can be written as

$$\dot{x} = Ax + B_1w + B_2u \quad (2.44a)$$

$$\chi = C_1x + D_{12}u \quad (2.44b)$$

$$y = C_2x + D_{21}w \quad (2.44c)$$

where

$$C_1 = \begin{pmatrix} Q^{1/2}/\ell \\ 0 \end{pmatrix} \quad D_{12} = \begin{pmatrix} 0 \\ I \end{pmatrix}$$

An \mathcal{H}_2 controller relates the measurements y and the control u such that when applied to the plant controls the evolution of the state x so as to minimise the cost functional $\mathcal{J}_{LQG}(\chi)$. We state a result

as found in [Lewis & Syrmos \(1995\)](#), in that the \mathcal{H}_2 controller which minimises \mathcal{J}_{LQG} can be found as a combination of optimal controller and the Kalman-Bucy filter. The estimator is given by the equation

$$u = -K\hat{x} \quad (2.45a)$$

$$\dot{\hat{x}} = A\hat{x} + B_2u - L(y - C_2\hat{x}) \quad (2.45b)$$

Where

$$K = -B_2^T X \quad X = \text{Ric} \begin{pmatrix} A & -B_2B_2^T \\ -C_1^T C_1 & -A^T \end{pmatrix} \quad (2.46a)$$

$$L = -Y^T C_2^T \quad Y = \text{Ric} \begin{pmatrix} A^T & -C_2C_2^T \\ -B_1B_1^T & -A \end{pmatrix} \quad (2.46b)$$

One observes the separation structure of the solution in that the computation of the control gain K_2 does not depend on the external disturbances which are taken care of by the terms B_1 and C_2 . Similarly the estimation gain L does not depend on the cost functional which are taken care of by the term C_1 or the way the state is measured as accounted for by B_2 , thus resulting in a decoupling of the problem for control and estimation, which is usually referred to as the principle of separation.

2.5 \mathcal{H}_∞ control: robust control

The formulation of the \mathcal{H}_∞ is similar to the \mathcal{H}_2 controller, only difference is that one considers the worst disturbance which destabilises the system, rather than a Gaussian disturbance. The governing equation are similar to the system of equation (2.44) and can be written as

$$\dot{x} = Ax + B_1w + B_2u \quad (2.47a)$$

$$\chi = C_1x + D_{12}u \quad (2.47b)$$

$$y = C_2x + D_{21}w \quad (2.47c)$$

in that one replaces the Gaussian disturbance w with the worst case disturbance w which destabilises the system. One considers the transfer function $\mathcal{T}_{\chi w}$ of the perturbation w which is obtained by solving the estimator problem for the feedback law χ . In an \mathcal{H}_∞ control one tries to bound the ∞ norm of the transfer function to be less than a chosen value γ i.e. $\|\mathcal{T}_{\chi w}\|_\infty < \gamma$, where γ is a constant and $\|\cdot\|_\infty$ is the infinity norm of the transfer function and as defined in [Zhou et al. \(1996\)](#)

$$\|\mathcal{T}_{\chi w}\|_\infty = \sup_{\omega} \sigma_{\max}(\mathcal{T}_{\chi w})(j\omega) \quad (2.48)$$

where σ_{max} corresponds to the largest singular value. The objective functional for minimisation can be written as

$$\mathcal{J}_\infty = E[x^T Qx + \ell^2 u^T u - \gamma^2 w^T w]$$

and the control u is chosen to minimise \mathcal{J}_∞ , while simultaneously finding the maximal external disturbance κ which destabilises the system. Thus the \mathcal{H}_∞ control is termed as a min-max problem. As in the previous section the covariance matrices G_1 and G_2 which characterises the system disturbances and the measurement disturbances are assumed to be known. As described in [Lewis & Syrmos \(1995\)](#) the \mathcal{H}_∞ controller minimises \mathcal{J}_∞ for the worst possible disturbance κ and is given by

$$u = -K_\infty \hat{x} \quad (2.49a)$$

$$\dot{\hat{x}} = A\hat{x} + B_2 u - L_\infty (y - C_2 \hat{x}) \quad (2.49b)$$

where the controller feedback K_∞ and the estimator feedback L_∞ are given by

$$K_\infty = -B_2^T X_\infty \quad X_\infty = \text{Ric} \begin{pmatrix} A & \gamma^{-2} B_1 B_1^T - B_2 B_2^T \\ -C_1^T C_1 & -A^T \end{pmatrix} \quad (2.50a)$$

$$L_\infty = -Y_\infty C_2^T \quad Y_\infty = \text{Ric} \begin{pmatrix} A^T & \gamma^{-2} C_1 C_1^T - C_2 C_2^T \\ -B_1 B_1^T & -A \end{pmatrix} \quad (2.50b)$$

The case of a LQG controller of \mathcal{H}_2 theory is obtained as a limit of $\gamma \rightarrow \infty$. Also the terms $\gamma^{-2} B_1 B_1^T - B_2 B_2^T$ and $\gamma^{-2} C_1 C_1^T - C_2 C_2^T$ need not be necessarily negative definite, so a solution of the Riccati equation exist for sufficiently large values of γ . The smallest value of $\gamma = \gamma_0$ for which the solution exist is determined numerically. For $\gamma > \gamma_0$ the controller is termed as suboptimal. Also another important thing is that contrary to the \mathcal{H}_2 formulation the control and state estimation are coupled in the \mathcal{H}_∞ formulation, as the computation of state feedback gain K_∞ depends on the covariance of state disturbances which are handled by the term B_1 , and the estimator gain L_∞ , depending on the weights of the cost functional which are accounted for in C_1 . In comparison the \mathcal{H}_∞ controller performs better than the \mathcal{H}_2 in terms of the stability.

Regarding the application of feedback control an extensive survey has been provided in [Kim & Bewley \(2007\)](#). Estimation based feedback control for spatially developing flows has been studied by [Chevalier et al. \(2007\)](#). Optimal and Robust control of channel flow in the presence of normal magnetic fields has been studied by [Debbagh et al. \(2007\)](#). Application of feedback control to cavity flows using reduced order modelling has been performed by [Samimy et al. \(2007\)](#). Recent developments includes the work of [Bagheri et al. \(2009a\)](#) who propose the use of balanced modes to obtain a reduction in the dimensionality of the full Navier Stokes equation and then design a feedback controller. Extension of the control design to the case of a spatially developing flows has been studied by [Bagheri et al. \(2009b\)](#) for the case of the linear complex Ginzburg-Landau equations. The use of global modes to perform control studies for the case of cavity flow has been studied by [Barbagallo et al. \(2009\)](#). Feedback control for the flow around a bluff body has been studied by [Pastoor et al. \(2008\)](#), and more recently [Weller et al. \(2009a\)](#). [Ahuja & Rowley \(2009\)](#) have studied the flow past a flat plate by constructing a reduced order model for the stable reduced order space of the Navier-Stokes equation which is determined using global unstable eigenmodes, and then designing an LQG control to stabilise the flow. Application of robust control has been

studied by [Zuccher *et al.* \(2004\)](#) for boundary layers and [Gavarini *et al.* \(2005\)](#) for the case of pipe flows. Application of feedback control to the linearised Navier-Stokes equation by solving a low dimensional Riccati equation, which corresponds to the dimension of the unstable subspace is found in the work of [Raymond & Thevenet \(2009\)](#). This approach is similar in principle to model reduction in terms of the reduction in the dimensionality of the Riccati equation being solved, but is different in that we seek a control for the high fidelity system. Other work include the application of the feedback control to study the flow around the flat plate, around a stationary state, in the presence of perturbations which has implications in turbulence control as in [Buchot & Raymond \(2009a\)](#), [Buchot & Raymond \(2009b\)](#).

2.6 Conclusions

To conclude this chapter is basically a glossary introduction to the various terms in the control literature which will be frequently used in this thesis. Control of a dynamical system can be basically classified as open loop or closed loop depending on the output observation of the response. The constrained optimisation technique based on the method of Lagrange multipliers has been described. The determination of functional gradients is accomplished through a sensitivity based approach and an adjoint based approach. The adjoint based method of determining the gradients can be further classified as discretise-differentiate, differentiate-discretise based on the order in which the differentiation is applied, the two approaches are not commutative.

The closed loop control also known as the feedback control has been discussed. Closed loop control is basically used when there are disturbances in the physical system, due to the presence of uncertainties and when open-loop control fails to give the desired effect. It is based on the concept of being able to monitor the model by means of output measurements and establishes a connection between the measurements and the input of the system. This involves the solution of an estimation problem. Based on the functional space setting in which the control is determined the feedback control can be classified as an \mathcal{H}_2 or a \mathcal{H}_∞ problem. The \mathcal{H}_2 is based on minimising a quadratic functional and can be further classified as an LQR or an LQG feedback control. In LQR control we assume that the external disturbances do not influence the plant dynamics and the states are estimated accurately. In the presence of external Gaussian noise the control is termed as an LQG. LQG control is equivalent to coupling of a LQR problem and a Kalman filter for estimation. The principle of separation ensures that the plant dynamics and observer dynamics are uncoupled. The \mathcal{H}_∞ is similar to the \mathcal{H}_2 controller, only difference being that one considers the worst disturbance which destabilises the system, rather than a Gaussian disturbance. This results in the solution of a min-max problem in which one tries to find a control which minimises the cost functional subjected to the maximisation of the external disturbance. Also the principle of separation is no longer valid as in case of \mathcal{H}_∞ control. In terms of the stability the \mathcal{H}_∞ controller performs better than the \mathcal{H}_2 controller.

Lire
la seconde partie
de la thèse